aggregation of BCG and reduced expression of several proteins in hypoxic condition as well, suggesting a role of MDP1 in regulation of gene expression in dormant bacilli. In addition to the role in the cytoplasm, MDP1 is exported by unknown mechanism to the cell wall and control the mycolic acid transfer [18] and mycobacterial adherence to lung epithelial cells [19]. Thus, MDP1 is a pleiotropic protein which has strong impacts on the mycobacterial virulence.

MDP1 has been also reported to be one of immunocompetent antigens. Prabhakar et al. [20] identified this protein as an immunodominant protein in human healthy contacts with TB patients through T-cell blot assay. They designated this protein as histone-like protein of Mtb (HLP_{Mt}), which is the same molecule as MDP1. Matsumoto et al. [21] found that CpG DNA enhances immunogenicity of MDP1, such as productivity of TNF-α and IL-6 from mouse macrophages. They showed that co-immunization of BALB/c and C3H/He mice with MDP1 and Mtb DNA elicited IFN-γ production specific for this protein and caused reduction of the bacterial burden following Mtb challenge [21].

DNA vaccination with gene gun bombardment is a reliable method to induce reproducible T-cell responses [22] and has been used for identification of T-cell epitopes of Mtb antigens, antigen (Ag) 85A [23–25], Ag85B [25], Ag85C [25], MPT51 [26,27], and *DosR* regulon-encoded proteins [28]. Here, we identified murine T-cell epitopes on MDP1 with a strategy using inbred mouse strains, gene gun immunization with expression plasmid DNA encoding MDP1, overlapping synthetic peptides spanning the entire mature MDP1 amino acid (aa) sequence, and major histocompatibility complex (MHC) binding peptide prediction algorithms.

2. Materials and methods

2.1. Animals

Inbred mouse strains, BALB/c, C57BL/6, and C3H/He, were purchased from Japan SLC (Hamamatsu, Japan). The mice were kept under specific pathogen-free conditions and fed autoclaved food and water *ad libitum* at the Institute for Experimental Animals of the Hamamatsu University School of Medicine. Two to three-month-old female mice were used in all experiments. Animal experiments were performed according to the Guidelines for Animal Experimentation, Hamamatsu University School of Medicine.

2.2. Plasmid

The DNA encoding MDP1 molecule was inserted between EcoRI and XhoI sites located downstream of cytomegalovirus immediate-early enhancer/promoter region of eukaryotic expression plasmid, pCI (Promega, Madison, WI, USA). The integrity of the nucleotide sequence was validated by automated DNA sequencing with ABI PRISM 310 genetic analyzer (Applied Biosystems, Foster City, CA, USA) using a dye primer cycle sequencing kit (Applied Biosystems).

2.3. Peptides

Peptides spanning the entire MDP1 aa sequence of BCG (205 aa residues) were synthesized as 20-mer peptides overlapping by 10 residues, with the exception of P6 (p46–65) and the carboxyl-terminal P21 (p186–205) ([15], Fig. 1). MDP1 p23–31 and p46–60 peptides were synthesized by Hayashi kasei (Osaka, Japan). All peptides were dissolved in phosphate-buffered saline (PBS) at a concentration of 10 mg ml^{-1} and stored at −80 °C until use.

2.4. Prediction of T-cell epitopes by MHC binding peptide prediction algorithms

For the prediction of murine T-cell epitopes, following MHC binding peptide prediction algorithms were used through their web sites. These are, National Institutes of Health BioInformatics and Molecular Analysis Section (BIMAS) ([29], http://bimas.dcrt.nig.gov/cgi-bin/molbio/ken_parker_comboform), SYFPEITHI program ([30], http://www.syfpeithi.de/), and RANKPEP program ([31], http://bio.dfci.harvard.edu/Tools/rankpep.html).

2.5. Immunization of mice

For DNA immunization with Helios gene gun system (Bio-Rad Laboratories, Hercules, CA, USA), preparation of the cartridge of DNA-coated gold particle cartridge was followed to the manufacturer's instruction manual. Finally, 0.5 mg of gold particles was coated with 1 μg of plasmid DNA and the injection was carried out with 0.5 mg gold per shot once. Mice were injected with 1 μg of plasmid DNA four times at 1-week intervals. Mice were also immunized subcutaneously with 10^6 CFU of BCG (Tokyo strain) twice at a 2-week interval.

2.6. Preparation of splenocyte culture supernatants

Spleen cells were harvested from mice. Recovered cells were cultured with RPMI medium supplemented with 10% fetal calf serum in 96-well plates at 2×10^6 cells/well in the presence or absence of 5 μg ml^{-1} of each MDP1 peptide at 37 °C with 5% CO_2 atmosphere. Supernatants were harvested 48 h later and stored at −20 °C until they were assayed. Concentration of IFN-γ in the culture supernatants was determined by a sandwich enzyme-linked immunosorbent assay (ELISA)

2.7. Quantification of IFN-γ with ELISA

The 96-well ELISA plates (EIA/RIA Plate A/2; Costar, Cambridge, MA) were coated with 2 μg ml^{-1} of capture antibody (Ab) (anti-murine IFN-γ monoclonal Ab [mAb] R4-6A2; BD Biosciences, San Jose, CA, USA) at 4 °C overnight, washed with PBS supplemented with 0.05% Tween 20 (PBS-Tween), and blocked with Block One Blocking solution (Nacalai Tesque, Kyoto, Japan) at room temperature for 45 min. After washed with PBS-Tween, the culture

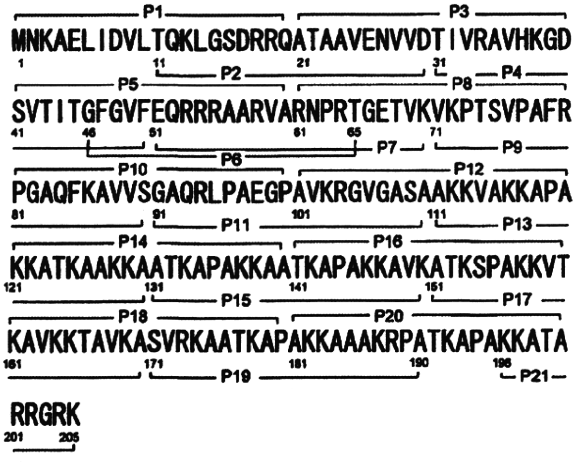

Fig. 1. Schematic representation of the 21 overlapping synthetic peptides from MDP1 of BCG. All peptides covering entire MDP1 of BCG (205 aa residues) were synthesized as 20-mer molecules overlapping by 10 amino acids with the neighboring peptides.

supernatants were added to the plates and the plates were incubated at 4 °C overnight. After washed with PBS-Tween, 0.5 μg ml^{-1} of biotin-labeled anti-murine IFN-γ mAb XMG1.2 (BD Biosciences) was added to the plates, and the plates were incubated for 1 h at room temperature. After washed with PBS-Tween, horseradish peroxidase-conjugated avidin (Bio-Rad Laboratories) was added and incubated for 30 min at room temperature. After washed, the plates were added with TMB one component HRP microwell substrate (BioFX Laboratories, Owings Mills, MD, USA) to detect bound horseradish peroxidase-conjugated streptavidin. After 5 min, the absorbance of each well was measured at 630 nm using an EZS-ABS Microplate Reader (Asahi Techno Glass Tokyo, Japan).

2.8. Depletion of CD4+ or CD8+ T-cell subsets

CD4+ or CD8+ T-cell subsets of peptide-reactive T-cells were determined by depletion of CD4+ or CD8+ T-cells, respectively. We used BD IMag system (BD Biosciences). Briefly, spleen cells were mixed thoroughly with anti-mouse CD4 particles-DM or anti-mouse CD8a particles-DM (BD Biosciences, 50 μl particles for 10^7 cells) and placed at 4 °C for 30 min. The labeled cells were placed on the BD IMagnet and incubated for 8 min. Supernatant was carefully removed. This supernatant contains the cell fraction which is devoid of CD4+ or CD8+ T-cells.

2.9. MHC stabilization assay

MHC stabilization assay is originally described in Ljunggren et al. [32]. RMA-S cells ([33], 10^6 cells/well) were cultured at 26 °C overnight and were then incubated for 1 h in the presence or absence of peptide (10, 50, or 100 μM). The cells were then transferred to 37 °C for 2 h and washed with FACS buffer, and cell surface expression of H2-D^b molecules was detected by flow cytometry by using phycoerythrin (PE)-conjugated mouse mAbs specific for H2-K^{d}D^b (28-14-8; eBioscience, San Diego, CA, USA). The results were expressed as the mean fluorescence intensity (MFI) ratio, which was determined as follows: MFI ratio = (MFI observed in the presence of peptide at 37 °C − MFI observed in the absence of peptide at 37 °C)/(MFI observed in the absence of peptide at 26 °C) × 100 (%).

2.10. Statistics

Data from multiple experiments were expressed as the means ± S.E.M. Data were analyzed with Student's unpaired *t*-test. *p* value of 0.05 or less was considered significant.

3. Results

3.1. IFN-γ production in response to overlapping synthetic peptides from MDP1 by splenocytes of pCI-MDP1 DNA-immune mice

Splenocytes from mice immunized with DNA vaccine encoding MDPI (pCI-MDP1) were stimulated with the overlapping MDP1 peptides for 48 h and IFN-γ concentration of culture supernatants was measured by ELISA. As shown in Fig. 2A, robust IFN-γ production was observed in splenocytes from MDP1 DNA-immune C57BL/6 mice (H2^b haplotype) in the presence of peptides P3 (p21–40), P9 (p71–90), and P11 (p91–110). Similarly, significantly higher IFN-γ production from splenocytes of MDP1 DNA-immune BALB/c (H2^d haplotype) and C3H/He (H2^k haplotype) mice were observed in response to two peptides, P5 (p41–60), P6 (p46–65) and three peptides, P5 (p41–60), P13 (p111–130), and P16 (p141–160), respectively (Fig. 2B and C). In C3H/He mice, P11 (p91–110) and P12 (p101–120) could induce relatively high IFN-γ production, but the value was not statistically significant.

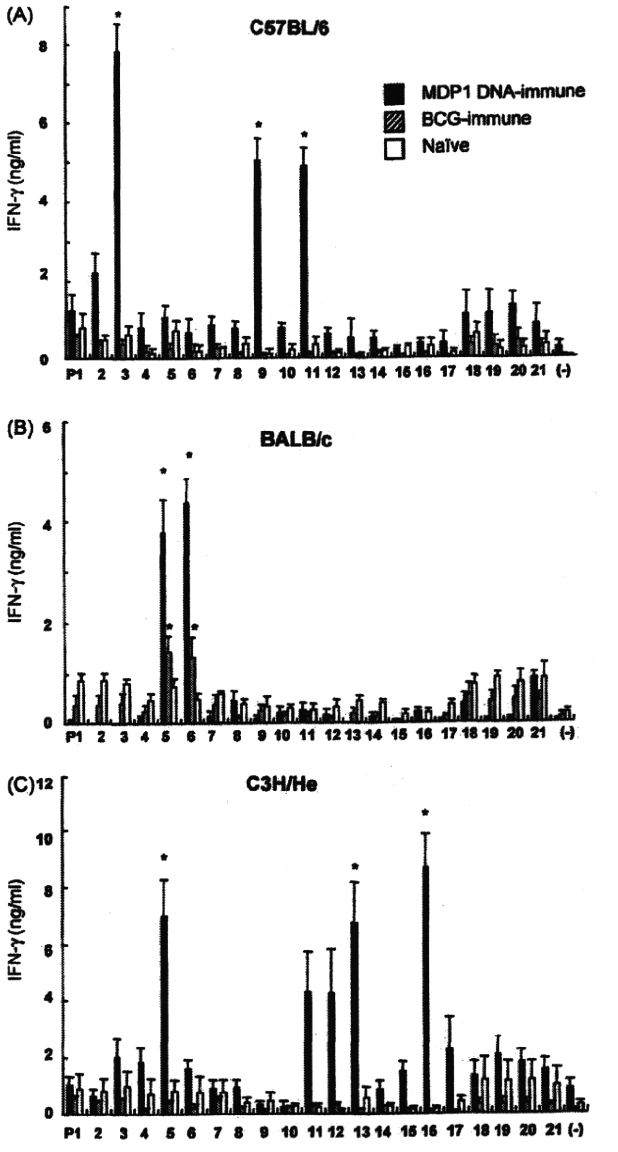

Fig. 2. IFN-γ production from splenocytes stimulated with overlapping peptides of MDP1. Inbred mice [C57BL/6 (A), BALB/c (B) and C3H/He (C)] were immunized with plasmid DNA encoding MDP1 using gene gun four times at 1-week intervals (filled bars) or with *M. bovis* BCG two times at a 2-week interval (hatched bars). The splenocytes (2×10^6) were stimulated with overlapping peptides (5 μg ml^{-1}) 2 weeks after the last immunization. Naïve mice (open bars) were used as controls. IFN-γ concentration of supernatant was analyzed by sandwich ELISA 48 h later. The means ± S.E.M. from three (C57BL/6, BALB/c) or six (C3H/He) mice are shown. Asterisks (*) indicate $p < 0.05$ compared with the value without peptide (-) with Student's unpaired *t*-test.

In order to examine whether the same peptide induce IFN-γ following natural mycobacterial infection, splenocytes from mice immunized with BCG were examined for IFN-γ production in response to MDP1 peptides. Two peptides, P5 and P6, also induced significant IFN-γ production from splenocytes of BCG-immune BALB/c mice (Fig. 2B), but the level of IFN-γ produced in BCG-immune mice was lower than that in MDP1 DNA-immune mice. We were not able to detect significant IFN-γ production from splenocytes of BCG-immune C57BL/6 and C3H/He mice (Fig. 2A and C). In this experimental condition, DNA immunization with MDP1 DNA was superior to BCG vaccination in terms of IFN-γ production level from splenocytes.

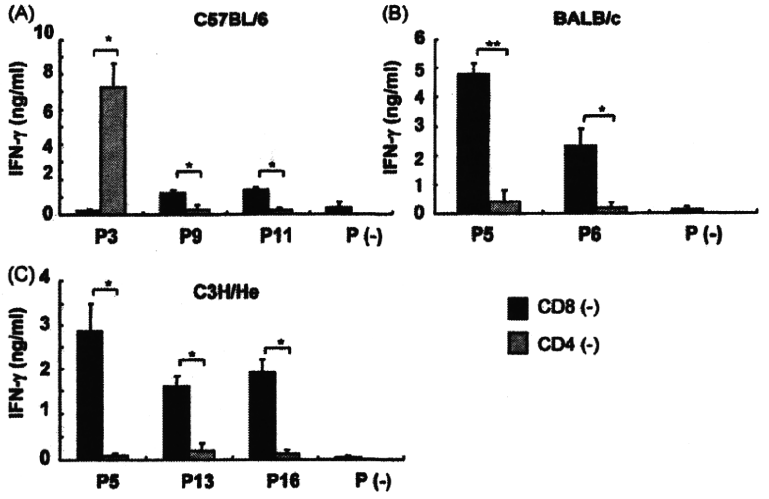

Fig. 3. Analysis of T-cell subsets responsive to MDP1 peptides. Mice were immunized with MDP1 DNA on the same schedule as Fig. 2. Splenocytes were treated with magnetic beads specific for CD4 or CD8. Cells (2×10^6) of the negative fraction were stimulated with peptides (5 μg ml^{-1}). Amounts of IFN-γ in the supernatant were analyzed by sandwich ELISA 48 h later. The mean ± S.E.M. of three mice are shown. $^{**}p < 0.01$, $^{*}p < 0.05$ (Student's unpaired *t*-test).

3.2. T-cell subset analysis of T-cells by the depletion of CD4+ or CD8+ T-cells

Next, we examined which T-cell subsets responding to MDP1 peptides. CD4+ or CD8+ T-cells were removed with magnetic beads and residual cells were stimulated with MDP1 peptides and resultant IFN-γ production was compared. As shown in Fig. 3A, IFN-γ production from splenocytes of C57BL/6 mice in response to P3 (p21–40) was significantly decreased by depleting CD8+ T-cell subset. In contrast, IFN-γ production in response to P9 (p71–90) and P11 (p91–110) was decreased by depleting CD4+ T-cells. These results indicate that P3 contains CD8+ T-cell epitope, and P9 and P11 contain CD4+ T-cell epitopes. Intracellular IFN-γ staining results showed that IFN-γ-producing CD8+, but not CD4+ T-cells were observed in response to P3 in C57BL/6 mice. And IFN-γ-producing CD4+, but not CD8+ T-cells were observed in response to P9 and P11 (data not shown). Since C57BL/6 mice have a deletion of H2-Eα gene and do not express H2-E molecules on the cell surface [34], two CD4+ T-cell epitopes in these peptides are exclusively considered to be presented on H2-A^b.

In BALB/c mice, IFN-γ production in the presence of P5 (p41–60) and P6 (p46–65) was significantly reduced by depleting CD4+ T-cells. Similarly, IFN-γ production in the presence of P5 (p41–60), P13 (p111–130), or P16 (p141–160) was significantly reduced by depleting CD4+ T-cells in C3H/He mice (Fig. 3B and C). These results indicate that these peptide regions contain CD4+ T-cell epitopes.

3.3. Identification of minimal T-cell epitopes in the responsive peptide regions of MDP1

Generally, CD8+ T-cells recognize peptides of 8–11 aa residues on MHC class I molecules and CD4+ T-cells recognize peptides of 12–18 aa residues on MHC class II molecules. Several MHC binding peptide prediction algorithms are available on internet.

Table 1
T-cell epitope candidates in MDP1 molecule.

Peptide	Amino acid sequence	Estimated scores for restriction molecules[a]	
		K^b	D^b
p21–40 (P3)	ATAAVENVVDTIVRAVHKGD		
p23–31 (9-mer)	AAVENVVDT	**0.13**	**108** 20
p23–32 (10-mer)	AAVENVVDTI	**0.40**	**50.2** 33
		A^d	E^d
p41–60 (P5)	SVTITGFGVFEQRRRAARVA		
p46–65 (P6)	GFGVFEQRRRAARVARNPRT		
p52–60	QRRRAARVA	11.9 (7.1)	–[b]
		A^k	E^k
p41–60 (P5)	SVTITGFGVFEQRRRAARVA		
p44–58 (15-mer)	ITGFGVFEQRRRAAR		24
GFGVFEQRR	10.8 (14.2)		
p111–130 (P13)	KKVAKKAPAKKATKAAKKAA	A^k	E^k
p113–121 (9-mer)	VAKKAPAKK	–	17.9 (10)
p116–124 (9-mer)	KAPAKKATK	–	25.4 (10)
p121–129 (9-mer)	KKATKAAKK	–	18.7 (10)
p141–160 (P16)	TKAPAKKAVKATKSPAKKVT	A^k	E^k
p142–150 (9-mer)	KAPAKKAVK	–	17.3 (10)
p145–153 (9-mer)	AKKAVKATK	–	15.9 (10)

Epitopes predicted by computer algorithms are shown.

[a] Estimated scores are derived from BIMAS (bold), SYFPEITHI (underlined), or RANKPEP (plain). Parentheses indicate threshold scores, scores above which suggest the peptide binding to the corresponding H2 molecule.

[b] Score not shown in the program.

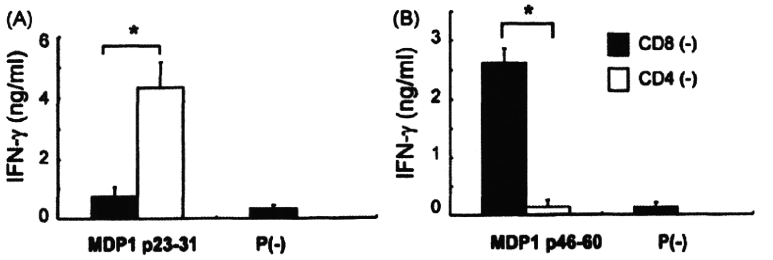

Fig. 4. IFN-γ production from T-cells in the presence of predicted peptides, MDP1 p23–31 and p46–60 peptides. C57BL/6 and BALB/c mice were immunized with MDP1 DNA and the immune splenocytes were treated with magnetic beads specific for CD4 or CD8α and purified the negative fraction. Cells (2×10^6) of the fraction were stimulated with 5 μg ml^{-1} of MDP1 p23–31 and MDP1 p46–65. IFN-γ in the culture supernatant was analyzed by sandwich ELISA 48 h later. The mean ± S.E.M. of three mice are shown. Asterisks (*) indicate $p < 0.05$ compared with the value without peptide (-) with Student's unpaired *t*-test.

We employed BIMAS and SYFPEITHI programs for prediction of CD8+ T-cell epitope(s) in P3 in C57BL/6 mice and RANKPEP program for CD4+ T-cell epitope(s) in P5 and P6 regions in BALB/c mice (Table 1). MDP1 p23–31 9-mer peptide (AAVENVVDT) in P3 region showed the highest score (108) for H2-D^b binding in BIMAS program (Table 1). In BALB/c mice, RANKPEP algorithm predicted MDP1 p52–60 as the core motif of H2-A^d-restricted CD4+ T-cell epitope (Table 1). Since both P5 (p41–60) and P6 (p46–65) peptides let the immune splenocytes produce IFN-γ, we prepared overlapping 15-mer peptide (p46–60) and examined the capacity to induce IFN-γ production from immune splenocytes.

As shown in Fig. 4A, CD8+ T-cells of MDP1 DNA-immune C57BL/6 mice produced significant amounts of IFN-γ in response to MDP1 p23–31 peptide. Splenocytes of the immune mice in the absence of the peptide and splenocytes of naïve C57BL/6 mice with or without the peptide did not produce significant level of IFN-γ (data not shown). Similarly, CD4+ T-cells of MDP1 DNA-immune BALB/c mice produced significant amounts of IFN-γ in response to MDP1 p46–60 peptide (Fig. 4B). Splenocytes of the immune mice in the absence of the peptide and splenocytes of naïve BALB/c mice with or without the peptide did not produce significant level of IFN-γ (data not shown). These results indicate that MDP1 p23–31 is a minimal *bona fide* CD8+ T-cell epitope in C57BL/6 mice and MDP1 p46–60 is CD4+ T-cell epitope in BALB/c mice, respectively.

As for C3H/He mice, RANKPEP program predicted that MDP1 p41–60 contains MDP1 p46–54 peptide which showed the highest score (10.8) in MDP1 peptides presented on H2-A^k. However, the score was less than the peptide binding threshold value (14.2), suggesting no binding. The SYFPEITHI program, which has the prediction program for H2-A^k and E^k, predicted MDP1 p44–58 15-mer peptide as H2-E^k binder with the highest score (24) in the program (Table 1). RANKPEP program also predicted three core 9-mer peptides restricted by H2-E^k, MDP1 p113–121, p116–124, and p121–129 in P13 (p111–130) region and two core peptides restricted by H2-E^k, MDP1 p142–150 and p145–153 in P16 (p141–160) region, respectively (Table 1).

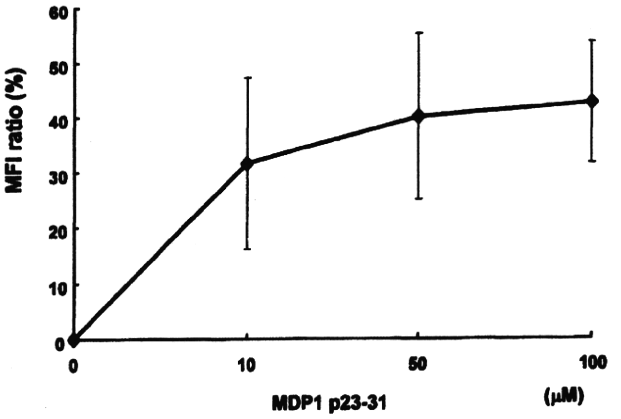

Fig. 5. MHC binding assay of MDP1 p23–31 to H2-D^b. The ability of MDP1 p23–31 for binding to H2-D^b was measured by determining the stabilization of class I molecules on the surfaces of TAP2-deficient RMA-S. RMA-S cells (10^6 cells/well) were cultured at 26 °C overnight and then were incubated for 1 h in the presence or absence of peptide (10, 50 or 100 μM). The cells were then transferred to 37 °C for 2 h and washed with FACS buffer, and cell surface expression of H2-D^b was detected by flow cytometry by using a phycoerythrin-conjugated mAb specific for H2-K^{d}D^b. The results were expressed as MFI ratio ± SD.

3.4. *Identification of an MHC class Ia restriction molecule for MDP1 p23–31 in C57BL/6 mice*

Since MDP1 p23–31 was found to be a CD8+ T-cell epitope for C57BL/6 mice, we examined MHC binding assay to determine H2 restriction molecule for the peptide. As shown in Fig. 5, the MFI ratio of PE-conjugated anti-H2-D^b mAb increased in the presence of 10 μM of MDP1 p23–31 peptide. This value further increased up to 42.5% in the presence of 100 μM of the peptide. This result confirmed that MDP1 p23–31 peptide does bind to H2-D^b.

4. Discussion

T-cells play pivotal role in induction of protective immunity against intracellular pathogens such as Mtb [6,7]. The protective immunity induced by MDP1 immunization would be mainly attributable to T-cell responses evoked by the immunization. We here determined murine T-cell epitopes of MDP1, which would give the concrete basis of the protective immunity by MDP1 immunization. The peculiar immunogenic feature of MDP1 is DNA-dependent augmentation of antigenicity. MDP1 elicited protective immune responses when it was vaccinated to BALB/c and C3H/He mice with genomic DNA derived from *M. tuberculosis* [21]. Up-regulation of antigen-presenting cell functions induced by the interaction between MDP1 and CpG DNA was suggested in the protective immune responses [21]. CpG DNA is a key component of DNA vaccines for evoking significant immune responses against antigens. Therefore, we considered that DNA vaccination of MDP1 induce substantial immune responses, because produced MDP1 proteins may bind to CpG DNA in plasmid backbone and enhance the adjuvant effects.

In this study, we found at least seven T-cell epitope candidates peptides upon MDP1 DNA immunization. By contrast, only one peptide region (MDP1 p41–65) was found with *M. bovis* BCG vaccination (Fig. 2B). Several reasons for this difference would be speculated. First, MDP1 localizes in the cytoplasmic space, or is tightly attached to the cell wall of the live *Mycobacterium*. Non-secreted antigens like MDP1 would be difficult to be immunoreactive in the form of BCG vaccine. Second, BCG vaccine has been reported to be

inefficient in terms of MHC class I antigen presentation. The fact may also cause the difference in the T-cell responses. Other possible explanation is that living mycobacteria have the mechanism to hide immunogenicity of MDP1, because strong immune response to MDP1 causes bactericidal host response.

In C57BL/6 mice, we found one CD8+ T-cell epitope, MDP1 p23–31 and two CD4+ T-cell epitopes, MDP1 p71–90 and MDP1 p91–110. MDP1 p23–31 (AAVENVVDT) was speculated to be presented on H2-D^b with prediction algorithms and this was confirmed with MHC binding assay. Reported dominant peptide binding motif of H2-D^b consists of asparagine at position 5 (P5) and hydrophobic C-terminal residue such as isoleucine or leucine (P9 or P10) [35,36]. P5 of MDP1 p23–31 is asparagine, but the C-terminal residue does not fit the motif. P5 (asparagine) and P10 (isoleucine) of MDP1 p23–32 fit the motif, suggesting that MDP1 p23–32 peptide also works as CD8+ T-cell epitope.

In BALB/c mice, MDP1 p46–60 was identified as H2-A^d-restricted CD4+ T-cell epitope. Since both P5 (p41–60) and P6 (p46–65) peptides, but not P7 (p51–70) peptide, let the immune splenocytes produce IFN-γ, we reasoned that the N-terminal aa residues (p46–50) are critical for the function. In C3H/He mice, at least three CD4+ T-cell epitopes were identified. RANKPEP or SYFPEITHI programs predicted P5 (p41–60), P13 (p111–130), and P16 (p141–160) bind to H2-E^k.

In conclusion, we identified murine T-cell epitopes of MDP1, an immunogenic major cellular mycobacterial protein causing protective immunity. We identified several CD4+ T-cell epitopes in three inbred mouse strains and one CD8+ T-cell epitope in C57BL/6 mice. Previously, we reported murine T-cell epitopes of MPT51, which is one of major secreted mycobacterial proteins at acute phase TB. MDP1 is a very abundant cellular protein and has been reported to be even up-regulated in dormant stage mycobacteria. Therefore, T-cell epitopes of MPT51 and MDP1 would be feasible for analysis of T-cell responses in different stage Mtb and for future TB vaccine design.

Acknowledgements

This work was supported by grants-in-aid for scientific research from the Japanese Society for the Promotion of Science (grant 20590438 to T. N. and grant 20390125 to Y. K.), a grant-in-aid for the Centers of Excellence (COE) Research Program from the Ministry of Education, Culture, Sports, Science and Technology of Japan, and a grant-in-aid from the United States-Japan Cooperative Medical Science Program.

References

[1] World Health Organization. WHO Report 2007 Global tuberculosis control: surveillance, planning, financing. Geneva; 2008 [online]. http://www.who.intentity/tb/publications/global_report/2008/pdf/fullreport.pdf (accessed 15.11.2008).
[2] Bloom BR, Fine PEM. The BCG experience: implications for future vaccines against tuberculosis. In: Tuberculosis: pathogenesis, protection, and control. Washington, DC: ASM Press; 1994. p. 531–57.
[3] Andersen P, Doherty TM. The success and failure of BCG—implications for a novel tuberculosis vaccine. Nat Rev Microbiol 2005;3:656–62.
[4] Sterne JAC, Rodrigues LC, Guedes IN. Does the efficacy of BCG decline with time since vaccination? Int J Tuberc Lung Dis 1998;2:200–7.
[5] Andersen P. Tuberculosis vaccines—an update. Nat Rev Microbiol 2007;5:484–7.
[6] Kaufmann SHE. How can immunology contribute to the control of tuberculosis? Nat Rev Immunol 2001;1:20–30.
[7] Kaufmann SHE. Immunity to intracellular bacteria. In: Paul WE, editor. Fundamental immunology. 5th ed. Philadelphia: Lippincott Williams & Wilkins Publishers; 2003. p. 1229–61.
[8] Kaufumann SHE, Flynn JL. CD8 T cells in tuberculosis. In: Cole ST, Eisenach KD, McMurray DN, Jacobs Jr WR, editors. Tuberculosis and the tubercle bacillus. Washington, DC: ASM Press; 2005. p. 465–74.
[9] Andersen P, Doherty TM. TB subunit vaccines—putting the pieces together. Microbes Infect 2005;7:911–21.
[10] Sable SB, Karlra M, Verma I, Khuller GK. Tuberculosis subunit vaccine design: the conflict of antigenicity and immunogenicity. Clin Immunol 2007;122:239–51.
[11] Park HD, Guinn KM, Harrell MI, Liao R, Voskuil MI, Tompa M, et al. Rv3133c/*dosR* is a transcription factor that mediates the hypoxic response of *Mycobacterium tuberculosis*. Mol Microbiol 2003;48:833–43.
[12] Karakousis PC, Yoshimatsu T, Lamichhane G, Woolwine SC, Nuermberger EL, Grosset J, et al. Dormancy phenotype displayed by extracellular *Mycobacterium tuberculosis* within artificial granulomas in mice. J Exp Med 2004;200:647–57.
[13] Matsumoto S, Yukitake H, Furugen M, Matsuo T, Mineta T, Yamada T. Identification of a novel DNA-binding protein from *Mycobacterium bovis* Bacillus Calmette-Guérin. Mirobiol Immunol 1999;43:1027–36.
[14] Lee BH, Murugasu-Oei B, Dick T. Upregulation of a histone-like protein in dormant *Mycobacterium smegmatis*. Mol Gen Genet 1998;260:475–9.
[15] Furugen M, Matsumoto S, Matsuo T, Matsumoto M, Yamada T. Identification of the mycobacterial DNA-binding protein 1 region which suppresses transcription in vitro. Microb Path 2001;30:129–38.
[16] Matsumoto S, Furugen M, Yukitake H, Yamada T. The gene encoding mycobacterial DNA-binding protein I (MDP I) transformed rapidly growing bacteria to slowly growing bacteria. FEMS Microbiol Lett 2000;182:297–301.
[17] Lewin A, Baus D, Kamal E, Bon F, Kunisch R, Maurischat S, et al. The mycobacterial DNA-binding protein I (MDPI) from *Mycobacterium bovis* BCG influences various growth characteristics. BMC Microbiol 2008;8:91–102.
[18] Katsube T, Matsumoto S, Takatsuka M, Okuyama M, Ozeki Y, Naito M, et al. Control of cell wall assembly by a histone-like protein in Mycobacteria. J Bacteriol 2007;189:8241–9.
[19] Aoki K, Matsumoto S, Hirayama Y, Wada T, Ozeki Y, Niki M, et al. Extracellular mycobacterial DNA-binding protein 1 participates in *Mycobacterium*-lung epithelial cell interaction through hyaluronic acid. J Biol Chem 2004;279:39798–806.
[20] Prabhakar S, Annapurna PS, Jain NK, Dey AB, Tyagi JS, Prasad HK. Identification of an immunogenic histone-like protein (HLP_{Mt}) of *Mycobacterium tuberculosis*. Tuberc Lung Dis 1998;79:43–53.
[21] Matsumoto S, Matsumoto M, Umemori K, Ozeki Y, Furugen M, Tatsuo T, et al. DNA augments antigenicity of mycobacterial DNA-binding protein 1 confers protection against *Mycobacterium tuberculosis* infection in mice. J Immunol 2005;175:441–9.
[22] Yoshida A, Nagata T, Uchijima M, Higashi T, Koide Y. Advantage of gene gun-mediated over intramuscular inoculation of plasmid DNA vaccine in reproducible induction of specific immune responses. Vaccine 2000;18:1725–9.
[23] Denis O, Tanghe A, Palfliet K, Jurion F, van den Berg TP, Vanonckelen A, et al. Vaccination with plasmid DNA encoding mycobacterial antigen 85A stimulates a $CD4^+$ and $CD8^+$ T-cell epitopic repertoire broader than that stimulated by *Mycobacterium tuberculosis* H37Rv infection. Infect Immun 1998;66:1527–33.
[24] Tanghe A, D'Souza S, Rosseels V, Denis O, Ottenhoff TH, Dalemans W, et al. Improved immunogenicity and protective efficacy of a tuberculosis DNA vaccine encoding Ag85 by protein boosting. Infect Immun 2001;69:3041–7.
[25] D'Souza S, Rosseels V, Romano M, Tanghe A, Denis O, Jurion F, et al. Mapping of murine Th1 helper T-cell epitopes of mycolyl transferases Ag85A, Ag85B, and Ag85C from *Mycobacterium tuberculosis*. Infect Immun 2003;71:483–93.
[26] Suzuki M, Aoshi T, Nagata T, Koide Y. Identification of murine H2-D^d- and H2-A^b-restricted T-cell epitopes on a novel protective antigen, MPT51, of *Mycobacterium tuberculosis*. Infect Immun 2004;72:3829–37.
[27] Aoshi T, Nagata T, Suzuki M, Uchijima M, Hashimoto D, Rafiei A, et al. Identification of an HLA-A*0201-restricted T-cell epitope on MPT51 protein, a major secreted protein derived from *Mycobacterium tuberculosis* by MPT51 overlapping peptide screening. Infect Immun 2008;76:1565–71.
[28] Roupie V, Romano M, Zhang L, Korf H, Lin MY, Franken KL, et al. Immunogenicity of eight dormancy regulon-encoded proteins of *Mycobacterium tuberculosis* in DNA-vaccinated and tuberculosis-infected mice. Infect Immun 2007;75:941–9.
[29] Parker KC, Bednarek MA, Coligan JE. Scheme for ranking potential HLA-A2 binding peptides based on independent binding of individual peptide side-chains. J Immunol 1994;152:163–75.
[30] Rammensee H-G, Bachmann J, Emmerich NPN, Bachor OA, Sevanović S. SYFPEITHI: database for MHC ligands and peptide motifs. Immunogenetics 1999;50:213–9.
[31] Reche PA, Glutting J-P, Zhang H, Reinherz EL. Enhancement to the RANKPEP resource for the prediction of peptide binding to MHC molecules using profiles. Immunogenetics 2004;56:405–19.
[32] Ljunggren HG, Stam NJ, Ohlen C, Neefjes JJ, Hglund P, Heemels MT, et al. Empty MHC class I molecules come out in the cold. Nature 1990;346:476–80.
[33] Ljunggren H-G, Kärre K. Host resistance directed selectively against H-2-deficient lymphoma variants. J Exp Med 1985;162:1745–59.
[34] Mathis DJ, Benoist C, Williams II VE, Kanter M, McDevitt HO. Several mechanisms can account for defective *Eα* gene expression in different mouse haplotypes. Proc Natl Acad Sci USA 1983;80:273–7.
[35] Rammensee H-G, Friede T, Stevanović S. MHC ligands and peptide motifs: first listing. Immunogenetics 1995;41:178–228.
[36] Margulies DH, McClusky J. The major histocompatibility complex and its encoded proteins. In: Paul WE, editor. Fundamental Immunology. 5th ed. Philadelphia: Lippincott Williams & Wilkins Publishers; 2003. p. 571–612.

IMMUNITY & AGEING

SHORT REPORT Open Access

Effectiveness of BCG vaccination to aged mice

Tsukasa Ito[1], Takemasa Takii[1*], Mitsuo Maruyama[2], Daisuke Hayashi[1], Takeshi Wako[2], Azusa Asai[2], Yasuhiro Horita[1], Keiichi Taniguchi[1], Ikuya Yano[3], Saburo Yamamoto[3], Kikuo Onozaki[1]

Abstract

Background: The tuberculosis (TB) still increases in the number of new cases, which is estimated to approach 10 million in 2010. The number of aged people has been growing all over the world. Ageing is one of risk factors in tuberculosis because of decreased immune responses in aged people. *Mycobacterium bovis* Bacillus Calmette Guérin (BCG) is a sole vaccine currently used for TB, however, the efficacy of BCG in adults is still a matter of debate. Emerging the multidrug resistant *Mycobacterium tuberculosis* (MDR-TB) make us to see the importance of vaccination against TB in new light. In this study, we evaluated the efficacy of BCG vaccination in aged mice.

Results: The Th1 responses, interferon-γ production and interleukin 2, in BCG inoculated aged mice (24-month-old) were comparable to those of young mice (4- to 6-week-old). The protection activity of BCG in aged mice against *Mycobacterium tuberculosis* $H_{37}Rv$ was also the same as young mice.

Conclusion: These findings suggest that vaccination in aged generation is still effective for protection against tuberculosis.

Introduction

The number of aged people has been increasing all over the world. World health organization reported that the increase rate of the number was 28% in the recent decade (2000 to 2009), and predicted that the number would reach 1.5 billion by 2050 [1]. The largest population of aged people (predicted to be 78% by the year 2050) resides in developing countries [1], where many infectious diseases, including tuberculosis (TB) [2], are endemic. Given the increased susceptibility of the elderly to infectious diseases, the rapid rise in the elderly population will become a significant threat to global health care.

The current TB vaccine is the live attenuated bacterium *Mycobacterium bovis* Bacillus Calmette Guérin (BCG). BCG is known to protect against tuberculous meningitis in babies children. However, it does not efficiently and consistently protect against pulmonary TB in adults. Over the years, many hypotheses have been put forward to explain the apparent variability in the protective efficacy of BCG, which varies from 0 to 80% [3]. Explanations for this inconsistency include differences in trial methodology, host population genetics, use of different BCG vaccine strains [4], and heterogeneous immunity to a variety of environmental mycobacteria that may interfere with the protection provided by BCG [5,6]. We have previously reported that 'early shared BCG strains' (ex. BCG-Russia, BCG-Moreau, BCG-Japan), which are chronologically early strains distributed form Pasteur Institute, conserve the characteristics of authentic BCG vaccine [7,8]. Immune response profiles following BCG vaccination comprise myriads of effecter mechanisms, multiple T-cell subsets, and many targeted antigens. BCG is capable of inducing Th1 responses [9], which are critical for protection against mycobacterial infection [10].

As an individual ages, significant immunological changes occur, which contribute to the enhanced morbidity and mortality associated with infectious diseases in the elderly. After puberty, thymic atrophy leads to a progressive decrease in the output of naïve T cells and decreased diversity in the T-cell repertoire [11]. $CD8^+$ T cells play an important role in innate response to pathogen such as *M. tuberculosis* in the aged mouse [12,13]. In this study, the efficacy of vaccination with BCG in aged mice was investigated.

* Correspondence: ttakii@phar.nagoya-cu.ac.jp
[1]Department of Molecular Health Sciences, Graduate School of Pharmaceutical Sciences, Nagoya City University, 3-1 Tanabe, Mizuho, Nagoya 467-8603, Japan
Full list of author information is available at the end of the article

Table 1 T cell subsets in the peripheral blood of young and aged mice [a]

	CD4	CD8	CD4/CD8
Young (4-6-week)	12.9 ± 6.55	17.3 ± 9.23	1.33 ± 0.66
Aged (24-month)	5.5 ± 1.83	6.2 ± 0.37	0.56 ± 0.28

[a] PBMC were stained with FITC-labeled anti-CD4 and PE-labeled anti-CD8 mAbs (BD Biosciences) and analyzed by FACScan. Data represent mean ± of three mice.

Results and Discussion

Specific-pathogen-free female C57BL/6 mice were supplied from the national center for geriatrics and gerontology (SLC, Japan). Young mice were 4- to 6-week of age, and old mice were 24-month of age. CD4/CD8 T cell ratio decreased by aging (Table 1), which is similar to previous reports [14,15]. Mice were vaccinated intraperitoneally with 10^6 colony forming unit (CFU) of *M. bovis* BCG Japan (Tokyo172) in 0.1 ml saline. The immunized mice were infected intravenously with 10^5 CFU *M. tuberculosis* strain $H_{37}Rv$ (ATCC 25618). To assess mycobacterial multiplication in spleen and lung, 0.1 ml of serial 10-fold dilutions of whole-organ 2-ml homogenates were plated onto Middlebrook 7H11 agar containing 10% OADC, and colonies were counted after 18-20 days post incubation at 37°C.

Th1 type cytokines are known to play an important role in the cellular type immune response in tuberculosis [16,17]. We investigated whether the Th1 cytokines were induced by BCG vaccination. The productions of interferon (IFN)-γ and interleukin (IL)-2 from splenocytes stimulated with purified protein derivatives (PPD) were elevated in both BCG vaccinated young (4- to 6-month-old) and aged mice (24-month-old), but not in non vaccinated mice (Figure 1). These results indicate that BCG vaccination can induce Th1 responses in aged mice comparable to young mice.

In order to avoid the effects of cytokines induced by BCG vaccination on infection of *M. tuberculosis*, the levels of cytokines (IL-6, IL-10, IL-12p70, monocyte chemotactic protein (MCP)-1, IFN-γ, tumor necrosis factor (TNF)-α) in the serum from BCG vaccinated young mice were measured by Cytometric Beads Array (CBA)

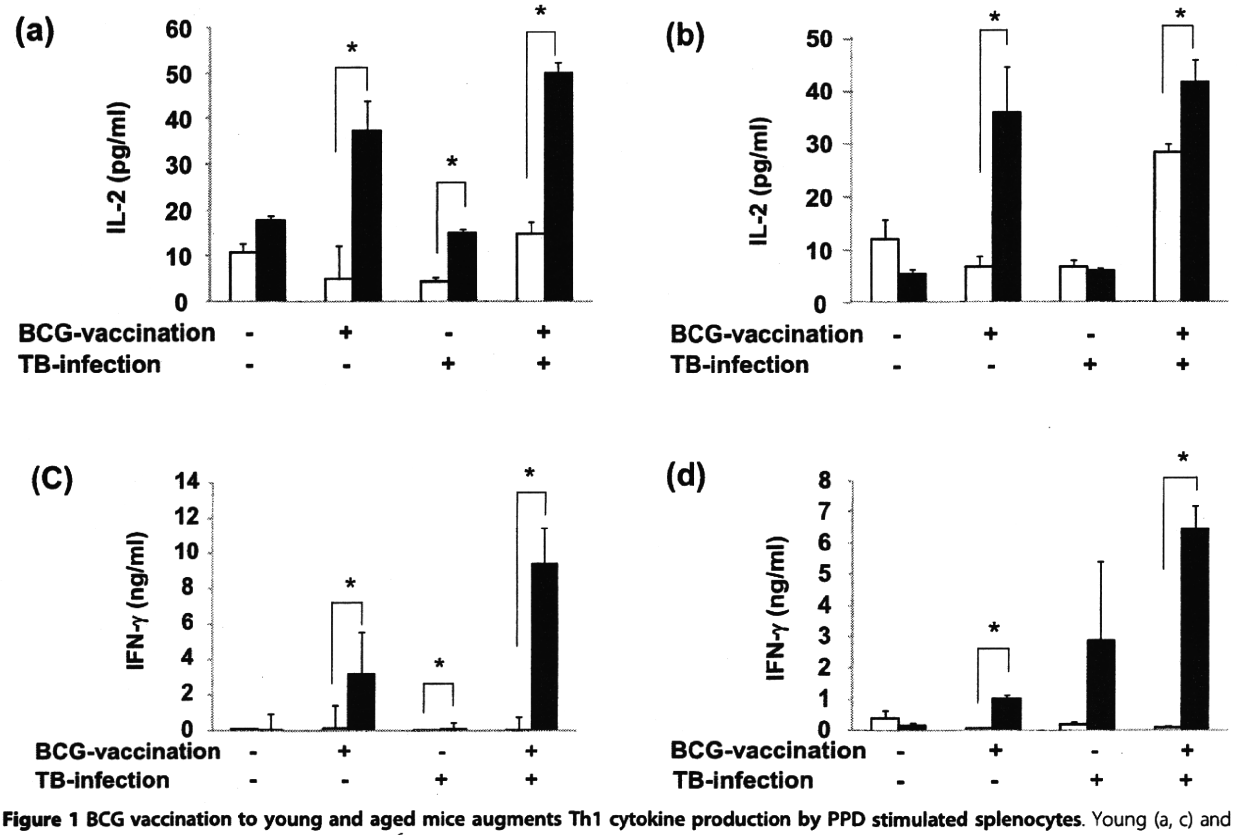

Figure 1 BCG vaccination to young and aged mice augments Th1 cytokine production by PPD stimulated splenocytes. Young (a, c) and aged (b, d) mice were immunized with 1 × 10^6 CFU of BCG or phosphate buffered saline (PBS). Eight weeks after immunization, the animals were intravenously challenged with 1 × 10^5 CFU of *M. tuberculosis* strain $H_{37}Rv$. Four weeks after challenge, the levels of IL-2 (a, b) and IFN-γ (c, d) in the culture supernatants of splenocytes stimulated with PBS (open column) or PPD (solid column) were measured by ELISA (BD Biosciences). Data represent mean ± SD of three mice. *, $p < 0.05$, compared with PBS-stimulation (student's *t*-test).

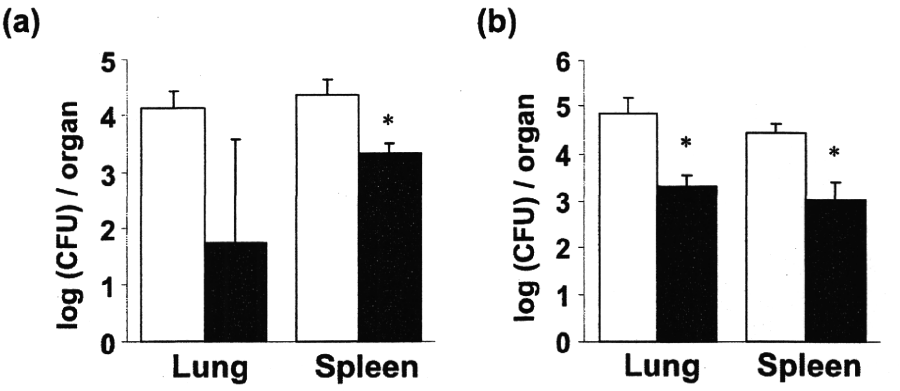

Figure 2 BCG protects both young and aged mice against *M. tuberculosis* infection. Young (a) and aged (b) mice were immunized with 1 × 10^6 CFU of BCG (solid column) or PBS (open column). Eight weeks after immunization, the mice were intravenously challenged with 1 × 10^5 CFU of *M. tuberculosis* strain $H_{37}Rv$. Four weeks after challenge, the bacterial numbers in the lung and spleen were determined by colony assay. Data represent mean ± SD of three mice. *, $p < 0.05$, compared with PBS-inoculated control group (student's *t*-test).

system (BD Biosciences, San Jose, CA). IL-10, IL-12 p70 and IFN-γ increased at 1 week post-inoculation, and returned to the basal level at 2 to 4 weeks. IL-6, TNF, MCP-1 peaked at two weeks after inoculation, and returned to the basal level at 4 weeks (data not shown). Therefore, the infection experiments were conducted six weeks after inoculation.

To confirm the inoculation of BCG and infection of *M. tuberculosis*, the level of serum antibody against PPD was measured by ELISA. The level of the antibody elevated two weeks after BCG inoculation, peaked at 4 weeks and returned to the basal level at 6 weeks. After infection of *M. tuberculosis* the level was elevated again (data not shown). Body weights of young mice slightly increased according to their growth, while those of aged mice slightly decreased (data not shown). The changes in body weight of young and aged vaccinated-mice were the same as those of non-vaccinated mice. Vaccinated mice grew normally, and death was not observed in both young and aged mice. Therefore, vaccination of BCG would be safe to both young and aged mice. Eight weeks after inoculation of BCG, mice were infected with *M. tuberculosis* $H_{37}Rv$ intravenously. Four weeks after infection the mice were killed and colony assay for bacterial count in the organs (lung and liver) from young and aged mice was performed (Figure 2). The bacterial numbers in both young and aged mice were reduced. These data indicate that BCG vaccination could induce the protection against *M. tuberculosis* in aged mice to the same degree as young mice.

Conclusion

In conclusion, this is a first report to evaluate the efficacy of BCG vaccination in aged (24-month-old) mice as compared to young (4- to 6-week-old) mice. BCG inoculation induced Th1 type immune responses in both young and aged mice (Figure 1). The protection activity was observed in aged mice, which was comparable to young mice (Figure 2). Our study suggests that vaccination in aged people could be effective to prevent infection against tuberculosis.

Abbreviations

TB: tuberculosis; BCG: *Mycobacterium bovis* Bacillus Calmette Guérin; IL: interleukin; MCP: monocyte chemotactic protein; INF: interferon; TNF: tumor necrosis factor; CFU: colony forming unit; PPD: purified protein derivatives.

Acknowledgements

This work was supported in part by Grant-in-Aid for Scientific Research on Kiban C from The Ministry of Education, Science, Sports, and a grant for Research on Publicly Essential Drugs and Medical Devices, KHC1021, KHC1016, from the Japan Health Sciences Foundation. We are grateful to Center for Experimental Animal Science, Nagoya City University Graduate School of Medical Sciences supporting the experiments involving the husbandry and management of laboratory animals.

Author details

[1]Department of Molecular Health Sciences, Graduate School of Pharmaceutical Sciences, Nagoya City University, 3-1 Tanabe, Mizuho, Nagoya 467-8603, Japan. [2]Department of Mechanism of Aging, Institute for Longevity Sciences, National Center for Geriatrics and Gerontology, 35 Gengo, Morioka, Obu, Aichi 474-8522, Japan. [3]Japan BCG Central Laboratory, 3-1-5 Matsuyama, Kiyose, Tokyo 204-0022, Japan.

Authors' contributions

TT, MM, and KO designed and planned the research. TI, TT, MM, TW, and AA performed the collection of serum and cytokine analysis. TI, DH, and YH performed infectious experiments and counting colonies of bacilli form infected organs. TI and KT performed FACS analysis. IY and SY supplied the BCG vaccine. All authors read and approved the final manuscript.

Competing interests

The authors declare that they have no competing interests.

Received: 13 June 2010 Accepted: 1 September 2010
Published: 1 September 2010

References

1. World Health Organization: **World Health Prospect.** World Health Organization, Geneva, Switzerland 2008 [http://esa.un.org/unpp/].
2. World Health Organization: **Global tuberculosis control-surveillance, planning, financing.** World Health Organization, Geneva, Switzerland 2008.
3. Fine PE: **Variation in protection by BCG: implications of and for heterologous immunity.** *Lancet* 1995, **346**:1339-1345.
4. Behr MA, Small PM: **Has BCG attenuated to importance?** *Nature* 1997, **389**:133-134.
5. Brandt L, Feino CJ, Weinreich OA, Chilima B, Hirsch P, Appelberg R, Andersen P: **Failure of *Mycobacterium bovis* BCG vaccine: some species of environmental mycobacteria block multiplication of BCG and induction of protective immunity to tuberculosis.** *Infect Immun* 2002, **70**:672-678.
6. Palmer CE, Long MW: **Effects of infection with atypical mycobacteria on BCG vaccination and tuberculosis.** *Am Rev Respir Dis* 1966, **94**:6553-6568.
7. Hayashi D, Takii T, Fujiwara N, Fujita Y, Yano I, Yamamoto S, Kondo M, Yasuda E, Inagaki E, Kanai K, Fujiwara A, Kawarazaki A, Chiba T, Onozaki K: **Comparable studies of immunostimulating activities in vitro among *Mycobacterium bovis* bacillus Calmette-Guérin (BCG) substrains.** *FEMS Immunol Med Microbiol* 2009, **56**:116-128.
8. Hayashi D, Takii T, Mukai T, Makino M, Yasuda E, Horita Y, Yamamoto R, Fujiwara A, Kanai K, Kondo M, Kawarazaki A, Yano I, Yamamoto S, Onozaki K: **Biochemical characteristics among *Mycobacterium bovis* BCG substrains.** *FEMS Microbiol Lett* 2010, **306**:103-109, 2010.
9. Vekemans J, Amedei A, Ota MO, D'Elios MM, Goetghebuer T, Ismaili J, Neport MJ, Prete GDel, Goldman M, McAdam KP, Marchant A: **Neonatal bacillus Calmette-Guerin vaccination induces adult-like IFN-γ production by $CD4^+$ T lymphocytes.** *Eur J Immunol* 2001, **31**:1531-1535.
10. Flynn J, Chan J: **Immunology of tuberculosis.** *Annu Rev Immunol* 2001, **19**:93-129.
11. Dominguez-Gerpe L, Rey-Mendez M: **Evolution of the thymus size in response to physiological and random events throughout life.** *Microsc Res Tech* 2003, **62**:464-476.
12. Posnett DN, Yarilin D, Valiando JR, Li F, Liew FY, Weksler ME, Szabo P: **Oligoclonal expansions of antigen-specific $CD8^+$ T cells in aged mice.** *Ann N Y Acad Sci* 2003, **987**:274-279.
13. Vesosky B, Rottinghaus EK, Davis C, Turner J: **CD8 T Cells in old mice contribute to the innate immune response to *Mycobacterium tuberculosis* via interleukin-12p70-dependent and antigen-independent production of gamma interferon.** *Infect Immun* 2009, **77**:3355-3363.
14. Jentsch-Ullrich K, Koenigsmann M, Mohren M, Franke A: **Lymphocyte subsets' reference ranges in an age- and gender-balanced population of 100 healthy adults–a monocentric German study.** *Clin Immunol* 2005, **116**:192-197.
15. Jiao Y, Qiu Z, Xie J, Li D, Li T: **Reference ranges and age-related changes of peripheral blood lymphocyte subsets in Chinese healthy adults.** *Sci China C Life Sci* 2009, **52**:643-650.
16. Salgame P: **Host innate and Th1 responses and the bacterial factors that control *Mycobacterium tuberculosis* infection.** *Curr Opin Immunol* 2005, **7**:374-380.
17. Doherty TM, Andersen P: **Vaccines for tuberculosis: novel concepts and recent progress.** *Clin Microbiol Rev* 2005, **18**:687-702.

doi:10.1186/1742-4933-7-12
Cite this article as: Ito *et al.*: **Effectiveness of BCG vaccination to aged mice.** *Immunity & Ageing* 2010 **7**:12.

INTERNAL MEDICINE

□ CASE REPORT □

A Case of Familial Pulmonary *Mycobacterium avium* Complex Disease

Masashi Matsuyama[1], Yukiko Miura[1], Takumi Kiwamoto[1], Ataru Moriya[1], Nariaki Kokuho[1], Kei Shimizu[1], Shigeo Otsuka[1], Minako Hijikata[2], Naoto Keicho[2], Kenji Hayashihara[1] and Takefumi Saito[1]

Abstract

We report one Japanese familial line in which there were three pulmonary MAC patients and one suspected patient over two generations, most of whom were diagnosed with the nodular/bronchiectatic type. In all patients, life circumstances and bacterial strains differed at the time of diagnosis. This suggests that the genes thought to affect patient susceptibility to pulmonary MAC disease may be involved in this family line. Comprehensive genotypic analysis of the *CFTR* gene, HLA typing, and analysis of the *NRAMP1* polymorphisms were performed in seven members of this family. The results suggest that female sex and menopause might be associated with onset of pulmonary MAC of the nodular/bronchiectatic type, and HLA-A26 antigen and diabetes mellitus might be involved in disease exacerbations.

Key words: familial pulmonary *Mycobacterium avium* complex disease, HLA-A26 antigen, menopause, *CFTR*, *NRAMP1*

(Inter Med 49: 949-953, 2010)
(DOI: 10.2169/internalmedicine.49.3023)

Introduction

Mycobacterium avium complex (MAC) lung disease is becoming increasingly prevalent, particularly the nodular/bronchiectatic type in patients with no pre-existing structural lung disease. Genetic defects have been suggested in familial cases; the sibling risk for nodular/bronchiectatic type pulmonary MAC is much higher than the population prevalence (1, 2).

Familial pulmonary MAC disease reports are very rare (2, 3). Most previous reports of pulmonary MAC disease susceptibility genes have been case-control studies of unrelated subjects, looking for polymorphisms in *HLA*, *CFTR*, and *NRAMP1* (4-11). To the best of our knowledge, this is the first report of familial pulmonary MAC disease with comprehensive genotypic analysis of the *CFTR* gene, HLA typing, and analysis of the *NRAMP1* polymorphisms. The present family included three patients and one suspected patient over two generations, most of whom had nodular/bronchiectatic type pulmonary MAC. Since each patient's life circumstances and bacterial strains differed at the time of pulmonary MAC diagnosis, genes or unknown factors affecting susceptibility to pulmonary MAC disease might have been involved. Thus, the clinical manifestations and genetic polymorphisms of the pulmonary MAC disease patients and healthy family members were analyzed to identify factors implicated in the development and exacerbation of pulmonary MAC disease.

Abbreviations: *NRAMP1*: natural resistance-associated macrophage protein, *CFTR*: cystic fibrosis transmembrane conductance regulator, HLA: human leukocyte antigen

Case Report

Figure 1 shows the family tree. The following individuals underwent detailed assessment: Case 1 (69-year-old woman, No. 1); Case 2 (No. 2), 2nd older sister of Case 1; sus-

[1]Department of Respiratory Medicine, National Hospital Organization, Ibaraki-Higashi National Hospital, Ibaraki and [2]Department of Respiratory Diseases, Research Institute, International Medical Center of Japan, Tokyo
Received for publication October 15, 2009; Accepted for publication January 28, 2010
Correspondence to Dr. Masashi Matsuyama, brwck573@yahoo.co.jp

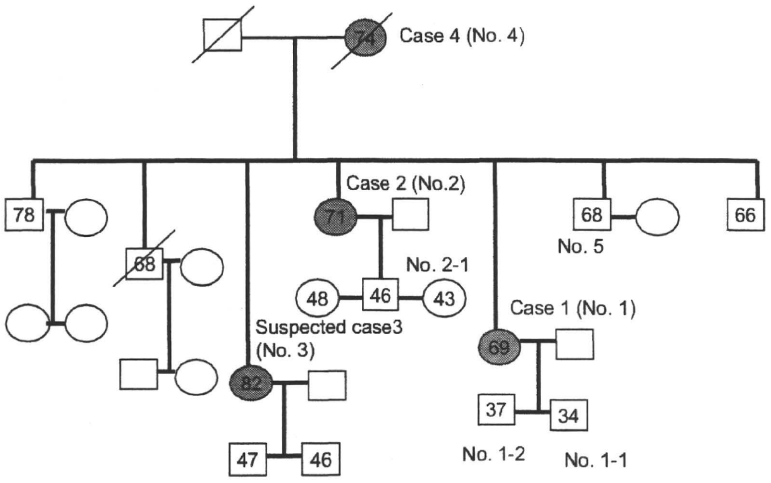

Figure 1. Family tree. Circles indicate females and squares refer to males. Numbers inside circles and squares indicate age (years) at the time of the present study. Gray symbols indicate those affected by pulmonary MAC, while white symbols refer to subjects unaffected by pulmonary MAC. Diagonal lines drawn through the symbols indicate deceased subjects.

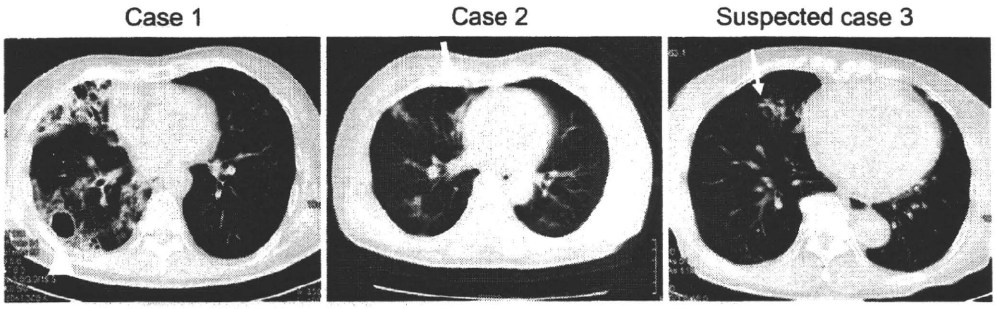

Figure 2. Computed tomography findings of Case 1, Case 2, and Case 3. Chest computed tomography (CT) scan demonstrates multiple, small, peripheral pulmonary nodules centred on the bronchovascular tree, cylindrical bronchiectasis, a cavitary lesion, and consolidations in Case 1 at the age of 69 years. The cavitary lesion, indicated by the arrowhead, resulted from expansion of the bronchiectatic lesion in Case 1. Multiple, small, peripheral, pulmonary nodules centred on the bronchovascular tree and cylindrical bronchiectasis are seen in Case 2, indicated by the arrow (at the age of 69 years). Nodular and centrilobular granular shadows are observed in Case 3, indicated by the thin arrow (at the age of 82 years). The CT scan findings of Case 1 are more severe than those of both Case 2 and Case 3.

pected Case 3 (No. 3), 3rd older sister of Case 1; younger brother of Case 1 (No. 5); two sons of Case 1 (No. 1-1 and No. 1-2); and a daughter of Case 2 (No. 2-1). Case 4 (No. 4), Case 1's mother, was deceased at the time of the study, but she had been diagnosed as having pulmonary MAC disease after menopause based on CT findings and sputum culture results.

Bacterial examination and chest CT findings confirmed nodular/bronchiectatic type pulmonary MAC disease in Cases 1 and 2 at 65 years of age. Chest CT showed nodular and centrilobular granular shadows in suspected Case 3 (Fig. 2); sputum cultures were negative, and bronchoscopic washing was not performed. It was thought that she might have pulmonary MAC disease associated with the same familial factors as her sisters and mother.

Delay in the time required for the taste of saccharin particles to be perceived was not observed in Case 1, Case 2, and suspected Case 3. Obstructive defects were not observed on pulmonary function testing, and elevated serum cold agglutinins were also not observed in any of the seven participating family members.

Standard commercial genetic mutation screening of the *CFTR* gene was performed in Case 1 (5); no known mutations and no novel variants were identified. The poly T polymorphisms in intron 8 (IVS8) of the *CFTR* gene were examined in all seven participating members (6). Three polymorphisms of the *NRAMP1* gene, the 5′(GT)n, D543N, and the 3′untranslated region TGTG insertion/deletion, were also genotyped in all seven family members (8). No significant differences between MAC cases and healthy members

Table 1. Characteristics of Individual Members of This Family Line

Family member (No.)	Age (at diagnosis ; years)	Sex	Diagnosis	Complication	HLA-A	*CFTR* polyT	*NRAMP1* D543N	*NRAMP1* TGTG
1 (case 1)	69 (65)	F (post memopausal)	Pulmonary *M.intracellulare*	Sinusitis DM endometriosis	26/26	7/7	G/G	ins/ins
1-1	34	M	-	-	26/24	7/7	G/G	ins/ins
1-2	37	M	-	-	26/24	7/7	G/G	ins/ins
2 (case 2)	71 (65)	F (post menopausal)	Pulmonary *M.avium*	Sinusitis	26/2	7/7	G/G	ins/ins
2-1	43	F (pre menopausal)	-	Sinusitis endometoriosis	26/24	7/7	G/G	ins/ins
3 (case 3)	82 (82)	F (post menopausal)	Suspected pulmonary MAC	Sinusitis	11/2	7/7	G/G	ins/ins
4 (case 4)	74 (N/A)	F (post menopausal)	Pulmonary MAC	N/A	N/A	N/A	N/A	N/A
5	68	M	-	-	26/2	7/7	G/G	ins/ins

HLA: human leukocyte antigen, *CFTR*: cystic fibrosis transmembrane conductance regulator, *NRAMP1*: natural resistance-associated macrophage protein one, MAC: *Mycobacterium avium* complex, DM: diabetes mellitus, N/A: not available, ins: insertion

were observed in the *NRAMP1* and *CFTR* gene polymorphisms. HLA typing showed that HLA-A26 antigen was predominant.

The characteristics of individual family members are shown in Table 1. All female family members had sinusitis, and all patients were postmenopausal females at the time of diagnosis.

Case 1 received combination chemotherapy (clarithromycin (CAM) 600 mg/day, ethambutol (EB) 750 mg/day, rifampin (RFP) 450 mg/day, and streptomycin (SM) 750 mg, 3 times a week for 3 months) because of productive cough. She continued to excrete MAC, and her CT findings worsened gradually despite adding levofloxacin (LVFX) 300 mg/day to her medication (Fig. 2, CT findings at 69 years of age). Case 1 had a history of diabetes mellitus (DM). Combination chemotherapy, including CAM (600 mg/day), EB (750 mg/day), and RFP (300 mg/day), was prescribed in Case 2. Although the patient continued to have positive sputum cultures, her symptoms and chest X-ray and CT findings showed little change with combination therapy. Since suspected case 3 was asymptomatic, she remained untreated. Drug susceptibility testing for *M. intracellulare* showed an MIC of 0.5 μg/mL for CAM in Case 1; in Case 2, the MIC of *M. avium* for CAM was 2.0 μg/mL. Case 1 had more severe symptoms and radiographic findings than Cases 2 and 3 (Fig. 2).

Abbreviation: MIC: minimal inhibitory concentration

Discussion

A familial study of the factors implicated in the development and exacerbation of pulmonary MAC disease, including testing for previously reported disease-susceptibility genes, was conducted in two pulmonary MAC cases, one suspected case, and four healthy members of this family.

Recurrent urinary tract infections occur in many postmenopausal women. In addition to epithelial atrophy, estrogen deficiency can increase vaginal pH and alter the vaginal flora, changes which may predispose to urinary tract infection (12). On the other hand, nodular-bronchiectatic type pulmonary MAC disease is well-known to occur after menopause. Estrogen may play also some role in resistance to MAC infection (13) due to its effects on various immune functions, such as macrophage activity, natural killer cell activity, and T cell-mediated immunity (13). Since all of the patients in this family were postmenopausal females, these factors might have been associated with pulmonary MAC disease onset.

In this family, all females had maxillary sinusitis, suggesting that they had sinobronchial syndrome. Hence, impaired mucociliary clearance may have been associated with pulmonary MAC disease in the females of this family. Major

sinobronchial syndromes are classified into diffuse panbronchiolitis, primary ciliary dyskinesia, and cystic fibrosis. *CFTR* mutations appear to contribute to the susceptibility and pathogenesis of pulmonary nontuberculous mycobacteria (NTM) infection (5-7). CFTR protein is a cyclic adenosine monophosphatase-regulated chloride channel located in the apical membrane of epithelial cells. CFTR deletion impairs mucociliary clearance together with changes in the airway microenvironment, and it leads to a progressive cycle of infection and inflammation (6). Although CF incidence is very low in the Japanese population because of the rare possession of a typical delta F508 mutation of the *CFTR* gene (14), Mai et al reported associations between the IVS8 5T allele in the *CFTR* gene and pulmonary MAC infection in Japanese (6). However, the IVS8 5T alleles were not identified in this family. Also, the full *CFTR* gene analysis on the most severe patient (Case 1) revealed that neither known mutations nor novel variants were present. On the other hand, Ziedalski and Kim et al. reported that the prevalence of *CFTR* mutations in their pulmonary NTM cohort ranged from 36% to 50% in the United States (5, 7). Thus, the genetic background of pulmonary MAC disease may differ between Japanese and Caucasian populations.

In this family line, all seven participating members did not meet the diagnostic criteria for diffuse panbronchiolitis, because of the results of pulmonary function testing and the serum cold agglutinin results. As for primary ciliary dyskinesia, examinations of biopsies with electron microscopy were not performed, because the results of saccharin testing did not fulfill the diagnostic criteria for primary ciliary dyskinesia in Case 1, Case 2, and suspected Case 3.

The murine *Nramp-1* determines susceptibility to intracellular pathogens. The human homologue, *NRAMP1*, might be involved in susceptibility to pulmonary MAC infection (8). All members of this family were homozygotes for major alleles of the D543N and TGTG insertion/deletion polymorphism of the *NRAMP1* gene, which occurs in 70% to 80% of the Japanese population (8). As a result, the effect of these alleles in this family was unclear.

DM might be associated with deterioration of infection because of impaired cell-mediated immunity (15). Case 1, with DM, had more severe symptoms and radiographic findings than Cases 2 and 3, who did not have DM. Therefore, DM might contribute to the severity of pulmonary MAC disease.

HLA plays an important role in immune response; previous studies have shown that NTM lung disease is associated with HLA alleles (9-11). Kubo et al suggested that HLA A-26 antigen might be associated with deterioration of pulmonary MAC infection (9). Case 1, with homozygously expressed HLA-A26, had more severe symptoms and radiographic findings than Case 2, with heterozygously expressed HLA-A26. Case 2 had more severe symptoms and radiographic findings than Case 3 without HLA-A26. Therefore, HLA-A26 might play a role in the deterioration of pulmonary MAC infection.

HLA class I antigens present peptides from inside the cell, including viral peptides if present. These peptides are produced from digested proteins that are broken down in the proteasomes. The peptides are also generally small polymers, about 9 amino acids in length. If foreign peptides are present on cells with HLA class I antigens, cells containing foreign proteins will be attacked by cytotoxic T lymphocytes. In general, HLA class I antigens are expressed on all nucleated cells, while HLA class II antigens are expressed on most immune system cells. HLA class I antigens are classified into A, B, and C. Therefore, it is speculated that certain peptides within the respiratory epithelium presented by HLA-A26 induce HLA-A26-restricted cytotoxic T lymphocytes, and this immune reaction is associated with deterioration of pulmonary MAC disease. Further studies detailing the role of HLA-A26 in the pathogenesis of pulmonary MAC disease are needed.

In conclusion, female sex and menopause might be associated with the onset of nodular/bronchiectatic type pulmonary MAC in this family. HLA-A26 antigen and DM might be involved in disease exacerbation. Thus, it is important to monitor the currently premenopausal daughters of Case 2 because of their similar backgrounds.

References

1. Griffith DE, Aksamit T, Brown-Elliott BA, et al. An official ATS/IDSA statement: diagnosis, treatment, and prevention of nontuberculous mycobacterial diseases. Am J Respir Crit Care Med **175**: 367-416, 2007.
2. Tanaka E, Kimoto T, Matsumoto H, et al. Familial pulmonary *Mycobacterium avium* complex disease. Am J Respir Crit Care Med **161**: 1643-1647, 2000.
3. Inoue T, Tanaka E, Sakuramoto M, et al. Three sisters of pulmonary *Mycobacterium avium* complex disease. Kansenshogaku Zasshi **79**: 341-347, 2005 (in Japanese).
4. Sexton P, Harrison AC. Susceptibility to nontuberculous mycobacterial lung disease. Eur Respir J **31**: 1322-1333, 2008.
5. Kim RD, Greenberg DE, Ehrmantraut ME, et al. Pulmonary nontuberculous mycobacterial disease: prospective study of a distinct preexisting syndrome. Am J Respir Crit Care Med **178**: 1066-1074, 2008.
6. Mai HN, Hijikata M, Inoue Y, et al. Pulmonary *Mycobacterium avium* complex infection associated with the IVS8-T5 allele of the *CFTR* gene. Int J Tuberc Lung Dis **11**: 808-813, 2007.
7. Ziedalski TM, Kao PN, Henig NR, et al. Prospective analysis of cystic fibrosis transmembrane regulator mutations in adults with bronchiectasis or pulmonary nontuberculous mycobacterial infection. Chest **130**: 995-1002, 2006.
8. Tanaka G, Shojima J, Matsushita I, et al. Pulmonary *Mycobacterium avium* complex infection: association with *NRAMP1* polymorphisms. Eur Respir J **30**: 90-96, 2007.
9. Kubo K, Yamazaki Y, Hanaoka M, et al. Analysis of HLA antigens in *Mycobacterium avium-intracellulare* pulmonary infection. Am J Respir Crit Care Med **161**: 1368-1371, 2000.
10. Takahashi M, Ishizaka A, Nakamura H, et al. Specific HLA in

pulmonary MAC infection in a Japanese population. Am J Respir Crit Care Med **162**: 316-318, 2000.

11. Um SW, Ki CS, Kwon OJ, et al. HLA antigens and nontuberculous mycobacterial lung disease in Korean patients. Lung **187**: 136-140, 2009.

12. Caillouette JC, Sharp CF Jr, Zimmerman GJ, et al. Vaginal pH as a marker for bacterial pathogens and menopausal status. Am J Obstet Gynecol **176**: 1270-1275, 1997.

13. Tsuyuguchi K, Suzuki K, Matsumoto H, et al. Effect of estrogen on *Mycobacterium avium* complex pulmonary infection in mice. Clin Exp Immunol **123**: 428-434, 2001.

14. Yamashiro Y, Shimizu T, Oguchi S, et al. The estimated incidence of cystic fibrosis in Japan. J Pediatr Gastroenterol Nutr **24**: 544-547, 1997.

15. Plouffe JF, Silva J Jr, Fekety R, et al. Cell-mediated immunity in diabetes mellitus. Infect Immun **21**: 425-429, 1978.

Genes and Immunity (2010), 1–7

www.nature.com/gene

ORIGINAL ARTICLE

Association analysis of susceptibility candidate region on chromosome 5q31 for tuberculosis

C Ridruechai[1], S Mahasirimongkol[2,3], J Phromjai[2], H Yanai[2,4], N Nishida[5], I Matsushita[6], J Ohashi[7], N Yamada[2], S Moolphate[2], S Summanapan[8], C Chuchottaworn[9], W Manosuthi[10], P Kantipong[11], S Kanitvittaya[12], P Sawanpanyalert[3], N Keicho[6], S Khusmith[1] and K Tokunaga[5]

[1]*Department of Microbiology and Immunology, Mahidol University, Bangkok, Thailand;* [2]*TB/HIV Research Project, Research Institute of Tuberculosis, Japan Anti-Tuberculosis Association, Chiang Rai, Thailand;* [3]*National Institute of Health, Department of Medical Sciences, Ministry of Public Health, Nonthaburi, Thailand;* [4]*Department of Clinical Laboratory, Fukujuji Hospital, Japan Anti-Tuberculosis Association, Tokyo, Japan;* [5]*Department of Human Genetics, Graduate School of Medicine, University of Tokyo, Tokyo, Japan;* [6]*Department of Respiratory Diseases, Research Institute, International Medical Center of Japan, Tokyo, Japan;* [7]*Doctoral Programme in Life System Medical Sciences, Graduate School of Comprehensive Human Sciences, University of Tsukuba, Ibaraki, Japan;* [8]*Chiang Rai Provincial Health Office, Office of the Permanent Secretary, Ministry of Public Health, Chiang Rai, Thailand;* [9]*Chest Disease Institute, Department of Medical Services, Ministry of Public Health, Nonthaburi, Thailand;* [10]*Bamrasnaradura Infectious Diseases Institute, Department of Disease Control, Ministry of Public Health, Nonthaburi, Thailand;* [11]*Department of Medicine, Chiang Rai Regional Hospital, Ministry of Public Health, Chiang Rai, Thailand and* [12]*Chiang Rai Regional Medical Sciences Center, Department of Medical Sciences, Ministry of Public Health, Chiang Rai, Thailand*

Chromosome 5q31 spans the T helper (Th) 2-related cytokine gene cluster, which is potentially important in Th1/Th2 immune responses. The chromosome 5q23.2–31.3 has been recently identified as a region with suggestive evidence of linkage to tuberculosis in the Asian population. With the aim of fine-mapping a putative tuberculosis susceptibility locus, we investigated a family-based association test between the dense single nucleotide polymorphism (SNP) markers within chromosome 5q31 and tuberculosis in 205 Thai trio families. Of these, 75 SNPs located within candidate genes covering SLC22A4, SLC22A5, IRF1, IL5, RAD50, IL13, IL4, KIF3A and SEPT8 were genotyped using the DigiTag2 assay. Association analysis revealed the most significant association with tuberculosis in haplotypes comprising SNPs rs274559, rs274554 and rs274553 of SLC22A5 gene ($P_{Global} = 2.02 \times 10^{-6}$), which remained significant after multiple testing correction. In addition, two haplotypes within the SLC22A4 and KIF3A region were associated with tuberculosis. Haplotypes of SLC22A5 were significantly associated with the expression levels of RAD50 and IL13. The results show that the variants carried by the haplotypes of SLC22A4, SLC22A5 and KIF3A region potentially contribute to tuberculosis susceptibility among the Thai population.
Genes and Immunity advance online publication, 20 May 2010; doi:10.1038/gene.2010.26

Keywords: *chromosome 5q31; family-based association test; Thais; tuberculosis*

Introduction

Tuberculosis is a major burden for global public health, especially in developing countries. Infection with *Mycobacterium tuberculosis* does not always result in tuberculosis; approximately 10% of infected individuals will eventually develop clinical disease during their lifetimes.[1] The outcome of infection is determined by environmental factors, pathogen virulence and host immune response. Human genetic variations involving susceptibility to tuberculosis has initially been shown in twins in whom the concordance rate was higher in monozygotic than in dizygotic twins,[2] although reanalysis of such a survey indicated that environmental factors outweighed the importance of hereditary factors.[3] Several forward genetic approaches, including genome-wide linkage analysis and candidate gene approaches, have been applied in an attempt to map and elucidate the host susceptibility genes that contribute to controlling the immune response against *M. tuberculosis*.

Five genome-wide linkage studies have been performed to date. The first study identified the suggestive evidence of linkage to tuberculosis on chromosomes 15q11–13 and Xq26 in the Gambians and South Africans.[4] Subsequent fine-mapping of 15q11–13 locus in the same ethnicity revealed a 7-bp deletion in the *UBE3A* gene associated with tuberculosis ($P = 0.002$).[5] The positional candidate gene encoding CD40 ligand, *TNFSF5*, located on Xq26.3 was subsequently investigated, but no association with tuberculosis was found.[6] The second two-stage genome scan in Brazilians suggested linkage evidence in three regions 10q26.13, 11q12.3 and 20p12.1.[7] The focused linkage analysis in the candidate region of

Correspondence: Dr K Tokunaga, Department of Human Genetics, Graduate School of Medicine, University of Tokyo, 7-3-1 Hongo, Bunkyo-Ku, Tokyo 113-0033, Japan.
E-mail: tokunaga@m.u-tokyo.ac.jp
Received 30 September 2009; revised 6 January 2010; accepted 14 January 2010

the human chromosome 17q provided weak evidence of linkage in 17q11–21.[8] The strongest evidence of linkage was shown in the genome-wide scan conducted in Moroccan multiplex families,[9] in which a region of chromosome 8q12-13 was mapped as a major susceptibility locus for tuberculosis with non-parametric multipoint likelihood binomial logarithm (base 10) of odds score of 3.49 and a parametric logarithm (base 10) of odds score of 3.38 under a dominant model. The fourth genome-wide linkage study in South Africa and Malawi has implicated regions of 6p21–23 and 20q13.31–33 for tuberculosis susceptibility.[10] Fine-mapping of 20q13.31–33 provided association evidence of melanocortin 3 receptor (*MC3R*) and cathepsin Z (*CTSZ*) genes. Finally, the genome-wide single nucleotide polymorphism (SNP)-based linkage analysis in 93 affected sib-pairs localized a region with suggestive evidence of linkage to chromosome 5q23.2–31.3 among the Thai population (Z_{lr} score 3.01, logarithm (base 10) of odds score 2.29) and two regions on chromosome 17p13.3-13.1 and 20p13-12.3 showed linkage evidence in families with a younger age at the onset of tuberculosis (logarithm (base 10) of odds score 2.57 and 3.33, respectively).[11] Collectively, those findings imply that the allelic architecture of genetic susceptibility to tuberculosis is likely heterogeneous, partly explained by the genetic background of the studied population.

The suggestive evidence of linkage to the 5q region in Asians is of particular interest because the region spans the major T helper (Th) 2 cytokine gene cluster, which is potentially important for Th1/Th2 immune responses. This region has been identified as a susceptibility locus for various infectious and autoimmune diseases. The linkage and allelic association between *Plasmodium falciparum* blood infection levels and markers on chromosome 5q31–33 have also been reported.[12,13] The region has been found to harbor a susceptibility locus (SM1) controlling the infection intensity of *Schistosoma mansoni*.[14] In autoimmune diseases, the gene conferring susceptibility to Crohn's disease has been linked to chromosome 5q31[15] and an attempt to localize this region through linkage disequilibrium (LD) mapping identified a long-range haplotype (~250 kb) that was strongly associated with the disease.[16] The cytokine gene-rich 5q31–33 region in association with susceptibility to other inflammatory conditions had been reported in psoriasis, asthma and/or atopic phenotypes. The polymorphic *IL4* gene on chromosome 5q31 has a linkage and association with atopic dermatitis in Japanese nuclear families,[17] while the 5q31-32 region was confirmed as a susceptible locus for psoriasis.[18] Furthermore, a number of linkage analyses in ethnically diverse populations have identified the linkage signals on chromosome 5q31–33 with total serum IgE,[19] bronchial hyper-responsiveness[20] and asthma-related phenotypes (5q23-31).[21]

The prime candidate genes within this linkage region are a cluster of Th2-related cytokine genes important in immune regulation including *IL4, IL5, IL13, RAD50, KIF3A, SLC22A4* and *SLC22A5*. Interleukin-4 and interleukin-13 coordinated in various immune functions including induction of immunoglobulin class switching, synthesis of IgE and promoting the expression of chemokines, whereas interleukin-5 enhanced the production and survival of eosinophils.[22] Recently, a critical *cis*-regulatory element controlling Th2 cytokine expression has been identified in the 3′end of *Rad50*,[23] which acts as a locus control region for the expression of *IL4* and *IL13* genes. Association analysis on the SNP rs17166050, located in intron 4 of *RAD50*, showed a significant association with Crohn's disease.[24] Thus, the unidentified SNPs in the 5q31 region may influence variation of gene function among populations and contribute to the risk of Crohn's disease and other infections and inflammatory diseases. The activation of Th2 cytokine genes has been suggested to correlate with extensive tuberculosis disease.[25] Th2 cytokines were shown to inhibit autophagy, a dynamic process of subcellular degradation, thus impairing the ability of macrophages to kill mycobacteria.[26] In addition, the hyper-virulent Beijing family of *M. tuberculosis* strains that are predominant in east Asian, preferentially induced human monocytes to express Th2 cytokines.[27,28] Therefore, variations within this Th2 cytokine locus are reasonable candidates that might involve in the immunopathology of tuberculosis.

In this study, we attempted to fine-map a putative tuberculosis susceptibility locus on chromosome 5q31. A panel of SNP markers within chromosome 5q31 was developed and the family-based association between these SNP markers and tuberculosis was analyzed. The results provide evidence on the association of variants in *SLC22A4, SLC22A5* and *KIF3A* with tuberculosis.

Results

Of the 83 SNPs that were analyzed by the PBAT software and Haploview, 6 SNPs with evidence of deviation from the Hardy–Weinberg equilibrium (P-value <0.05) and 2 SNPs being monomorphic were excluded. Mendelian inconsistencies within families detected by PedCheck and Haploview were manually deleted. Pedigree errors among family members inspected by the Graphical Representation of Relationships (GRR) program were not observed partly because of the strong linkage disequilibria among the markers that were tested, resulting in none of the families being excluded. After the quality control process, 75 SNPs, which passed the specified criteria, were further analyzed. The genotyped SNPs within the candidate genes located on chromosome 5q31 covering *SLC22A4, SLC22A5, IRF1, IL5, RAD50, IL13, IL4, KIF3A* and *SEPT8* and their physical locations, are described in Supplementary Figure 1 and Supplementary Table 1. Linkage disequilibrium patterns across the 5q31 region were determined and 60 out of 75 SNPs were assigned into the six haplotype blocks (Supplementary Figure 1).

To examine the usefulness of the HapMap data for the association study on the 5q31 region, the patterns of LD in four populations, African (YRI), European (CEU), Chinese (CHB) and Japanese (JPT), were compared using genotype data from the HapMap and Thai trio families. In agreement with the earlier report,[29] we confirmed the similarity of LD patterns among the Chinese, Japanese and Thais in this 5q31 region.

Single marker and haplotype analyses

The associations of SNPs and haplotypes with tuberculosis under four different genetic models, additive,

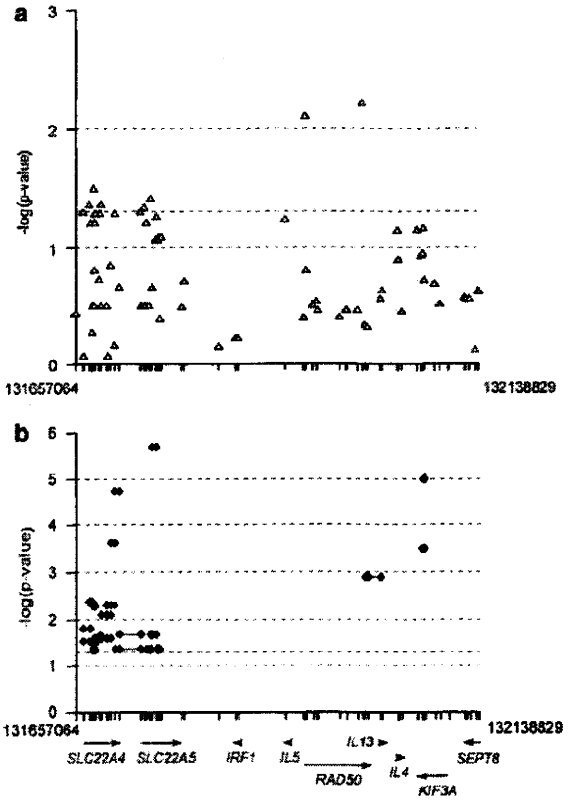

Figure 1 Association plots between single nucleotide polymorphisms (SNPs) located on chromosome 5q31 (NCBI Build 36) and tuberculosis. (a) The −log (*P*-values) plots for single-SNP association analysis were obtained from the best genetic model. (b) The global *P*-value plots for overall haplotype association analysis presented when $P<0.05$. The filled symbols connected by solid lines indicated the haplotype.

dominant, recessive and heterozygous advantage, were tested using the PBAT software. The SNPs with a *P*-value of <0.05 are detailed in Supplementary Table 2. Under the additive genetic model, the strongest association with tuberculosis for an individual marker, rs2237060, located on the *RAD50*, was shown ($P=0.0061$) (Figure 1a). Allele A of this A/C SNP was transferred from parents to offspring with tuberculosis. On the basis of the significant threshold at 1.74×10^{-4} estimated by taking into account the effective number of tests for single SNP analysis, the number of sliding windows for haplotype analysis and the number of genetic models included, this single-marker association evidence was not sufficient to reject the null hypothesis of no association with tuberculosis.

The most significant association with tuberculosis was observed in haplotype block 1 ($P_{Global}=2.02\times10^{-6}$) under the dominant model of inheritance as shown by association analysis of a three-marker haplotype present in each haplotype block (Figure 1b and Table 1). This haplotype is located within the *SLC22A5* gene comprising rs274559, rs274554 and rs274553 (Table 1). Significant global associations with tuberculosis were also detected in haplotypes of *SLC22A4* and *KIF3A* genes (rs272873-rs2306772-rs272867 and rs2299007-rs2237057-rs2299006, respectively) under the heterozygous advantage model of inheritance (Table 1). They remained significant after multiple testing correction (*P*-value $<1.74\times10^{-4}$).

Association analysis of the imputed untyped SNPs

A total of 895 imputed SNPs, including SNPs having association with Crohn's disease and psoriasis, were tested for association with tuberculosis. As expected, the imputation-based SNP analysis provided lower power to detect the disease association than those of typed SNPs. None of the imputed SNPs provided association evidence with tuberculosis after multiple testing corrections (Supplementary Table 3). However, the results of the imputed genotype and their frequencies can provide draft pictures of the association patterns between untyped SNPs and tuberculosis in the Thai population.

Effect of the associated haplotype on gene expression levels

To evaluate the possible effect of the significantly associated haplotype (rs274559, rs274554 and rs274553) on the expression of the neighboring genes, the UNPHASED software was used to test the association between this haplotype and the expression levels of *SLC22A4, SLC22A5, IRF1, IL5, RAD50, IL13, IL4, KIF3A, SEPT8 and PCDH1* derived from genomic expression microarray analysis of four populations, CHB, JPT, CEU and YRI, in the HapMap database. The haplotype was significantly associated with the *RAD50, IL13* and *PCDH1* expression (overall *P*-value $=6.14\times10^{-4}$, 6.70×10^{-4} and 1.90×10^{-4}, respectively) and remained significant after multiple testing correction (*P*-value <0.005 for 10 tests performed). Different expression levels of *RAD50, IL13* and *PCDH1* in various combinations of three SNP genotypes were shown (Supplementary Figure 2, 3 and 4). However, when this quantitative-trait locus analysis was restricted to only CHB+JPT, it became non-significant because of the limited number of haplotypes in each population. In addition, the frequencies of this significantly associated haplotype are quite similar among the CHB, JPT and Thais, but are totally different from those in the CEU/YRI (data not shown).

Discussion

Chromosome 5q31 has been suggested as the susceptibility loci of related inflammatory diseases in ethnically diverse populations, including tuberculosis among the Thais.[11] The region has been of particular interest because it carries a cluster of Th2 cytokines and related genes including *IL4, IL5, IL13, RAD50, KIF3A, SLC22A4* and *SLC22A5*. Such results have allowed us to conduct fine-mapping of the tuberculosis susceptibility locus in this region in Thai trio families. Here we report a nominal association with tuberculosis for individual SNPs located in *SLC22A4, SLC22A5* and *RAD50* genes, although none of them remained statistically significant after multiple testing correction. The failure to provide a significant association could be explained by small sample size resulting in insufficient power to detect genetic risks with small effect size. Moreover, the presenting linkage may be the results of the multiple causative alleles within the same linkage region as shown in Crohn's disease.[30] Therefore, replication in an

Table 1 Association between three-marker haplotypes and tuberculosis

SNP ID	*Gene symbol*	*Haplotype*	*Haplotype frequency*	*Fam#*	*I_P-value*[a] *(FBAT)*	*Power (FBAT)*	*G_P-value*[b] *(WaldI)*
rs272879-rs272873-rs2306772[c]	*SLC22A4*	GCG	0.3584	120	+0.8111	0.0779	2.41×10^{-4}
		CCG	0.1202	70	−0.0435	0.1854	
		GTG	0.0108	16	−0.4926	0.0500	
		CTG	0.1729	85	−0.7681	0.8788	
		GCA	0.3136	106	−0.0054	0.6161	
		CCA	0.0111	16	−0.3867	0.0500	
rs272873-rs2306772-rs272867[c]	*SLC22A4*	CGC	0.3644	123	+0.6783	0.0601	1.86×10^{-5}
		TGC	0.0102	13	+0.6941	0.0500	
		CAC	0.3155	105	−0.0070	0.5698	
		CGT	0.1141	65	−0.0631	0.1245	
		TGT	0.1729	87	−0.8448	0.8581	
		TAT	0.0100	14	−0.0758	0.8105	
rs274559-rs274554-rs274553[d]	***SLC22A5***	CGG	0.6738	50	−0.7942	0.2869	$\mathbf{2.02 \times 10^{-6}}$
		TGG	0.1987	91	−0.9387	0.0686	
		CAC	0.0177	15	+0.7380	0.1578	
		TAC	0.0993	64	−0.0751	0.2350	
rs3798132-rs2299007-rs2237057[c]	*KIF3A*	ATC	0.3551	112	−0.6137	0.0500	3.22×10^{-4}
		GTC	0.0454	31	−0.6748	0.0977	
		ACC	0.3932	101	+0.1689	0.4564	
		GTT	0.1828	78	−0.1768	0.1451	
rs2299007-rs2237057-rs2299006[c]	*KIF3A*	TCC	0.3482	114	−0.4487	0.0500	1.00×10^{-5}
		CCC	0.3870	103	+0.0767	0.3888	
		TCG	0.0542	37	−0.7473	0.0883	
		CCG	0.0135	12	+0.9724	0.1874	
		TTG	0.1802	77	−0.1799	0.1102	

Abbreviations: Fam#, number of informative families; FBAT, family-based association test; G_*P*-value, global *P*-value; I_*P*-value, individual *P*-value; SNP, single-nucleotide polymorphism. The most significant association with tuberculosis is shown in bold.
[a]Negative/positive signs represent the direction of association between individual haplotype and tuberculosis.
[b]Uncorrected *P*-value.
[c]Haplotype carried under a heterozygous advantage model of inheritance.
[d]Haplotype carried under a dominant model of inheritance.

independent population and study in a larger number of samples are needed to prove the association.

The observed associations of three-marker haplotype comprising SNPs of *SLC22A4*, *SLC22A5* and *KIF3A* with tuberculosis, which remained significant after multiple testing correction, suggested these are the reasonable candidate genes contributing to tuberculosis susceptibility. We avoid the false positives from population stratification by the family-based association study in which the majority of samples are complete trios. Despite the significant associations observed in this study, without replication study in other populations, false-positive findings cannot be refused at the moment.

Polymorphisms in *SLC22A4* and *SLC22A5* have been suggested to be associated with Crohn's disease in the Caucasians but the variants are extremely rare in Asians.[24,31] It is possible that the same locus can be involved in susceptibility to several related phenotypes as reported in this study on different variants in *SLC22A* and *SLC22A5* contributing to tuberculosis susceptibility. The genomic neighborhood surrounding the Th2 cytokine cluster is particularly important for their gene expression or activities.[22,23] Three SNPs comprising the most significant haplotype of *SLC22A5* are located in the intron and the bioinformatics prediction of these SNPs suggested their roles in gene expression. In light of this prediction, the quantitative association of this haplotype and the expression level of genes within the Th2 cytokine cluster region were determined and the results showed that this haplotype is associated with the expression levels of *IL13* and *RAD50*. As *RAD50* contains the locus control region regulating the Th2 cytokine expression, including *IL4* and *IL13*, it is possible that variation in *RAD50* could indirectly influence the fate or magnitude of T-cell responses to infectious agents such as *M. tuberculosis*. In addition, substantial evidence indicated that increased interleukin-4 production in tuberculosis is likely associated with immunopathology.[25,32]

The associated haplotype encompassing the *SLC22A4* ergothioneine transporter, *SLC22A5* L-carnitine transporter, and the *KIF3A* gene encoding for a subunit of kinesin II, a microtubule-based motility protein,[33] suggested their role in disease susceptibility. However, in the absence of a validated biological function in tuberculosis and with regard to the heterozygous advantage model for the associations of *SLC22A4* and *KIF3A* haplotypes, it could be speculated that these haplotypes might not have true biological effects, but they are proxies to primary, but untyped, markers nearby. The heterozygous advantage model of inheritance has been described in a number of genes including the *SLC6A4* serotonin transporter gene.[34] However, as heterosis at a molecular level seems contrary to the expectation for the degree of phenotypic effect, the presence of heterosis in *SLC22A4* and *KIF3A* genes remains to be clarified.

In summary, the observations from fine-mapping and gene expression analysis enable us to confine a region of potential risk markers and haplotypes for tuberculosis within chromosome 5q31. The variants in *SLC22A4*, *SLC22A5*, *KIF3A* or flanking genes, especially genes

containing master regulatory elements for Th2 cytokine expression, may have an important role in susceptibility to tuberculosis. However, to define the causative variants, replication studies in other Asian populations and/or functional analysis of associated variants require further investigations.

Materials and methods

Sample description

Of the 203 complete trios (parents and their affected offspring) and two incomplete trio families (father or mother and affected offspring) were recruited through the tuberculosis surveillance system in Chiang Rai, the northernmost province in Thailand. Of the 203 complete trio families, 15 were part of multi-case families in a previous linkage study.[11] Tuberculosis was diagnosed on the basis of clinical presentation and bacteriological confirmation by sputum culture for *M. tuberculosis* or at least two out of three positive sputum smears for acid-fast bacilli. Diagnosis of tuberculosis in a few cases was obtained from records in the tuberculosis surveillance system accompanied by a current abnormal chest x-ray. This study was reviewed and approved by the Ethics Review Committee for Research in Human Subjects, Ministry of Public Health, Thailand and the Institutional Review Board of the International Medical Center of Japan. All patients were tested for HIV using standard serological tests. HIV-infected patients were excluded from this study. Their blood samples were collected after obtaining individual informed consent.

Genotyping and quality control

Genomic DNA was extracted from the whole blood or peripheral blood mononuclear cells using QIAamp blood midi kit (Qiagen, Hilden, Germany). The tagging SNPs were randomly selected from a 610-kb region of 5q31–33. These markers were originally chosen for a fine-mapping study for various immune disorders associated with the 5q31 region, before the release of the HapMap data. Genotyping of 96 SNPs within chromosome 5q31 was performed by Digitag2 assay described earlier.[35] The genotype calls were determined by the visual inspection of cluster plot from the SNPStar software (version 0.0.0.8, Olympus, Tokyo, Japan). The successfully typed SNPs were analyzed by Haploview version 4.1.[36] SNP genotypes of the parent data set showing significant deviation from the Hardy–Weinberg equilibrium (P-value <0.05) and being monomorphic were excluded from further association test. Mendelian inconsistency within families was detected by PedCheck[37] and Haploview version 4.1. Genotyping errors within the family were deleted manually.

Relationship determination

Pedigree error should be suspected when a number of Mendelian inconsistencies are observed more often than expected by genotyping errors. Relatedness among family members was evaluated by Graphical Representation of Relationships (GRR) program.[38] As the studied markers are highly correlated, genotype information alone does not have the power to discriminate between pedigree error and genotyping error.

Family-based association study

Family-based association tests were analyzed by the PBAT software version 3.6.[39] Single marker and haplotype analyses were performed based on the conditional power calculations. Statistical parameters for testing the null hypothesis of no linkage and no association were family-based association test-GEE and four genetic models of inheritance, namely additive, dominant, recessive and heterozygous advantage models. The plots of uncorrected P-values from the association tests were created using snp.plotter.[40]

Bonferroni correction is overly conservative in this fine-mapping analysis because of high linkage disequilibrium patterns between the markers that were tested. Thus, SNP spectral decomposition[41] was used to calculate the effective number of tests that should be corrected for single SNP analyses and the P-value threshold for rejecting null hypothesis accounting for their highly correlated allelic structure. The experiment-wide significance threshold required to keep type I error rate at 5% from SNP spectral decomposition was 0.0021. However, this threshold did not consider the number of sliding windows for haplotype tests and did not allow correction for the various genetic models tested. Taking into account the 24 effective numbers of tests corrected for single SNP analysis, 48 three-marker sliding windows calculated from 60 SNPs in the defined haplotype blocks and four genetic models tested, 288 tests were performed. This resulted in threshold to maintain the type I error rate at 5% of $P<1.74\times10^{-4}$ for the multiple testing correction in this study.

The structures of LD determined by Haploview and the pairwise LD among genotyped SNPs were measured by r^2 values. Haplotype blocks were defined based on the method described earlier[42] and the individual and overall family-based haplotype association analyses were then performed according to the defined haplotype blocks. The LD structure in the YRI, CEU, CHB and JPT was determined using genotype data from the HapMap web site (http://www.hapmap.org).

Imputation of untyped SNPs in trio samples and the HapMap reference samples

Imputation was carried out by the PLINK version 1.04 based on the HapMap genotype data of 90 JPT + CHB individuals available on the PLINK website (http://pngu.mgh.harvard.edu/purcell/plink/).[43] Individual genotype data were in forward orientation with the NCBI Build 36 reference. To prevent the problem of strand flipping in C/G and A/T SNPs, the genotyped markers with these allele configurations were removed from the input data. Removing these SNPs resulted in 54 genotyped SNPs in the trio families used in the imputation. Imputation of untyped SNPs in the trio families was based on 895 SNPs extending from 131.5 to 132.3 Mb within the HapMap individual genotype data. The imputed data set was used for empirical assessment of allele frequency of untyped SNPs and the family-based association analysis by PLINK. The association analysis of imputed untyped markers should be considered as preliminary and results having lower power and accuracy than those of typed markers were expected. We aimed to use this imputed information to provide the empirical information for the untyped SNPs within the

5q31 region that is associated with other related diseases including Crohn's disease and psoriasis.

Bioinformatics prediction of SNPs' functions
The functional SNP (F-SNP) database[44] (http://compbio.cs.queensu.ca/F-SNP/) was accessed to retrieve the functional information of SNPs that showed the lowest *P*-value in the association analysis.

Analysis of SNP effects on gene expression
The expression data of the genes on chromosome 5q31 covering *SLC22A4, SLC22A5, IRF1, IL5, RAD50, IL13, IL4, KIF3A, SEPT8 and PCDH1* were retrieved from the GENEVAR web site (http://www.sanger.ac.uk/humgen/genevar/). These normalized data sets of gene expression were produced from genome-wide expression arrays (Sentrix Human-6 Expression BeadChip, Illumina Inc., San Diego, CA, USA) in the Epstein–Barr virus-transformed lymphoblastoid cell lines of 150 offspring in phase I and phase II of the HapMap Consortium (populations: YRI, CEU, CHB and JPT). The haplotype frequencies among these populations were also determined with Haploview version 4.1. The haplotypes showing a significant association with tuberculosis were assessed for the effects on gene expression using UNPHASED version 3.0.13.[45] The box plots representing normalized expression levels of genes in various combinations of three-SNP genotypes were created with R software version 2.7.2 (http://www.r-project.org/).

Conflict of interest

The authors declare no conflict of interest.

Acknowledgements

This study was partly supported by International Cooperation Research grant, the Ministry of Health, Labor and Welfare from 2002 to 2004 and by a grant-in-aid for scientific research on priority areas 'Comprehensive Genomics' from the Ministry of Education, Culture, Sports, Science and Technology of Japan and intramural grant from Department of Medical Sciences, Ministry of Public Health, Thailand. We thank all staffs and collaborators of the TB/HIV research project, Thailand, a collaborative research project between the Research Institute of Tuberculosis (RIT) and the Japan Anti-tuberculosis Association, and the Department of Medical Sciences, Ministry of Public Health for collecting the clinical information and samples.

References

1 Bloom BR, Small PM. The evolving relation between humans and *Mycobacterium tuberculosis*. *N Engl J Med* 1998; **338**: 677–678.
2 Comstock GW. Tuberculosis in twins: a re-analysis of the Prophit survey. *Am Rev Respir Dis* 1978; **117**: 621–624.
3 van der Eijk EA, van de Vosse E, Vandenbroucke JP, van Dissel JT. Heredity versus environment in tuberculosis in twins: the 1950s United Kingdom Prophit Survey Simonds and Comstock revisited. *Am J Respir Crit Care Med* 2007; **176**: 1281–1288.
4 Bellamy R, Beyers N, McAdam KP, Ruwende C, Gie R, Samaai P *et al*. Genetic susceptibility to tuberculosis in Africans: a genome-wide scan. *Proc Natl Acad Sci USA* 2000; **97**: 8005–8009.
5 Cervino AC, Lakiss S, Sow O, Bellamy R, Beyers N, Hoal-van Helden E *et al*. Fine mapping of a putative tuberculosis-susceptibility locus on chromosome 15q11-13 in African families. *Hum Mol Genet* 2002; **11**: 1599–1603.
6 Campbell SJ, Sabeti P, Fielding K, Sillah J, Bah B, Gustafson P *et al*. Variants of the CD40 ligand gene are not associated with increased susceptibility to tuberculosis in West Africa. *Immunogenetics* 2003; **55**: 502–507.
7 Miller EN, Jamieson SE, Joberty C, Fakiola M, Hudson D, Peacock CS *et al*. Genome-wide scans for leprosy and tuberculosis susceptibility genes in Brazilians. *Genes Immun* 2004; **5**: 63–67.
8 Jamieson SE, Miller EN, Black GF, Peacock CS, Cordell HJ, Howson JM *et al*. Evidence for a cluster of genes on chromosome 17q11-q21 controlling susceptibility to tuberculosis and leprosy in Brazilians. *Genes Immun* 2004; **5**: 46–57.
9 Baghdadi JE, Orlova M, Alter A, Ranque B, Chentoufi M, Lazrak F *et al*. An autosomal dominant major gene confers predisposition to pulmonary tuberculosis in adults. *J Exp Med* 2006; **203**: 1679–1684.
10 Cooke GS, Campbell SJ, Bennett S, Lienhardt C, McAdam KP, Sirugo G *et al*. Mapping of a novel susceptibility locus suggests a role for MC3R and CTSZ in human tuberculosis. *Am J Respir Crit Care Med* 2008; **178**: 203–207.
11 Mahasirimongkol S, Yanai H, Nishida N, Ridruechai C, Matsushita I, Ohashi J *et al*. Genome-wide SNP-based linkage analysis of tuberculosis in Thais. *Genes Immun* 2009; **10**: 77–83.
12 Rihet P, Traore Y, Abel L, Aucan C, Traore-Leroux T, Fumoux F. Malaria in humans: *Plasmodium falciparum* blood infection levels are linked to chromosome 5q31-q33. *Am J Hum Genet* 1998; **63**: 498–505.
13 Flori L, Kumulungui B, Aucan C, Esnault C, Traore AS, Fumoux F *et al*. Linkage and association between *Plasmodium falciparum* blood infection levels and chromosome 5q31-q33. *Genes Immun* 2003; **4**: 265–268.
14 Marquet S, Abel L, Hillaire D, Dessein A. Full results of the genome-wide scan which localises a locus controlling the intensity of infection by *Schistosoma mansoni* on chromosome 5q31-q33. *Eur J Hum Genet* 1999; **7**: 88–97.
15 Rioux JD, Silverberg MS, Daly MJ, Steinhart AH, McLeod RS, Griffiths AM *et al*. Genomewide search in Canadian families with inflammatory bowel disease reveals two novel susceptibility loci. *Am J Hum Genet* 2000; **66**: 1863–1870.
16 Rioux JD, Daly MJ, Silverberg MS, Lindblad K, Steinhart H, Cohen Z *et al*. Genetic variation in the 5q31 cytokine gene cluster confers susceptibility to Crohn disease. *Nat Genet* 2001; **29**: 223–228.
17 Kawashima T, Noguchi E, Arinami T, Yamakawa-Kobayashi K, Nakagawa H, Otsuka F *et al*. Linkage and association of an interleukin 4 gene polymorphism with atopic dermatitis in Japanese families. *J Med Genet* 1998; **35**: 502–504.
18 Friberg C, Bjorck K, Nilsson S, Inerot A, Wahlstrom J, Samuelsson L. Analysis of chromosome 5q31-32 and psoriasis: confirmation of a susceptibility locus but no association with SNPs within SLC22A4 and SLC22A5. *J Invest Dermatol* 2006; **126**: 998–1002.
19 Marsh DG, Neely JD, Breazeale DR, Ghosh B, Freidhoff LR, Ehrlich-Kautzky E *et al*. Linkage analysis of IL4 and other chromosome 5q31.1 markers and total serum immunoglobulin E concentrations. *Science* 1994; **264**: 1152–1156.
20 Postma DS, Bleecker ER, Amelung PJ, Holroyd KJ, Xu J, Panhuysen CI *et al*. Genetic susceptibility to asthma–bronchial hyperresponsiveness coinherited with a major gene for atopy. *N Engl J Med* 1995; **333**: 894–900.